ELECTRIC FIELD INDUCED TRANSFORMATION TO HIGHLY CONDUCTING STATE IN ION-EXCHANGED OXIDE GLASSES CONTAINING Bi_2O_3
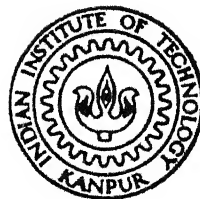
By

TOM MATHEWS

MATERIALS SCIENCE PROGRAM

ADVANCED CENTRE FOR MATERIALS SCIENCE

INDIAN INSTITUTE OF TECHNOLOGY, KANPUR

APRIL, 1987

ELECTRIC FIELD INDUCED TRANSFORMATION TO HIGHLY CONDUCTING STATE IN ION-EXCHANGED OXIDE GLASSES CONTAINING Bi_2O_3

A Thesis Submitted
In Partial Fulfilment of the Requirements
for the Degree of
MASTER OF TECHNOLOGY

By
TOM MATHEWS

to the

MATERIALS SCIENCE PROGRAM

ADVANCED CENTRE FOR MATERIALS SCIENCE

INDIAN INSTITUTE OF TECHNOLOGY, KANPUR

APRIL, 1987

MSP- 1987 -M- MAT- ELE

CERTIFICATE

This is to certify that the thesis entitled 'ELECTRIC FIELD INDUCED TRANSITION TO HIGHLY CONDUCTING STATE IN LITHIUM OXIDE GLASSES CONTAINING Bi_2O_3' by Tom Mathews is carried out under my supervision and has not been submitted elsewhere for a degree.

D. Chakravorthy
Professor
Materials Science Programme

ACKNOWLEDGEMENTS

CONTENTS

LIST OF TABLES

LIST OF FIGURES

Glasses have been known to be solid electrolytes for a long time. Recent advances in the development of Fast Ion Conducting glasses (FIC) have opened up many new applications including high energy density batteries, electrochromic displays and sensors. Most of such FIC glasses are based on compositions derived from silver iodide. Highest conductivity is exhibited by FICs based on silver ion migration. Only very few of the FIC glasses are based on SiO_2 tetrahedra as the network former because of the problem of silver precipitating out as metallic agglomerates during the melting process. Large concentrations of silver ions can be injected into SiO_2 based glasses by subjecting the glass fibers to sodium $\rightleftharpoons$ silver ion-exchange treatment well below the glass transition temperature. The electrical properties of such glass fibers has been reported by Chakraverty, 1986.

In the present thesis the effect of silver rich layers induced by subjecting the glass in the bulk form [3 mm^3 size] to sodium $\rightleftharpoons$ silver ion-exchange well below the glass transition temperature, on the electrical properties is studied.

Chapter I deals with the electrical conductivity (both ionic and electronic) of glasses and literature survey. In this chapter electrical properties, models and mechanism for ionic and electronic conduction in glasses along with AC and DC responses of various glass systems are discussed. Various aspects of ion-exchange and a brief review on FIC glasses are also incorporated.

Chapter II describes the experimental techniques used for the preparation and characterization of the various glasses investigated. The characterization techniques include AC and DC electrical conductivity measurements and X-ray analysis.

Chapter III deals with AC and DC resistivities of certain glasses in the bulk form based on the SiO_2 tetrahedral frame work containing Bi_2O_3 with varying amounts of Na_2O (10-30 mole %). These glasses after ion-exchange show lowering of resistivity and activation energy. An optimum combination of electrical field and temperature brings about a permanent morphological transformation presumably in the ion-exchanged layer inducing a high conductivity. The newly attained high conducting state is characterized by activation energies tending to zero. Such behavior has been attributed to the microstructural features of the ion-exchanged (silver rich) layer. It appears that the conduction in the newly formed state is ionic in nature.

Chapter IV gives a summary of the results obtained in the present investigation.

Chapter I

INTRODUCTION

Ion transport in glasses has been the subject of study since 1884 when Warburg [1] showed that sodium can be transported through Thuringer glass from one sodium-amalgam bath to another by the application of a DC voltage across the glass envelop. Haber and Moser [2] in 1905 reported the use of Thuringer glass to measure the partial pressure of oxygen in a CO/CO_2 mixture. Hauffe [3] used in an electrochemical cell, sodium conducting glasses to monitor activity of sodium in sodium-mercury amalgams. Development of glasses with higher ionic conductivities had been slow till last decade since the mechanisms of ion transport in glasses were not understood clearly due to the difficulty in defining the local glass structure and the inability to effectively isolate carrier and mobility contribution to conductivity [4]. In late 1960s and in the 1970s people discovered unusually high ionic conductivity in a number of crystalline materials. A remarkable advance in this field took place in 1967 when Kummar and Weber [5] of Ford Motor Co. reported high sodium ion conduction in sodium β-alumina · a two dimensional fast ion conductor. With the development of the sodium β-alumina-sodium-sulfur cell a number of limitations

associated with the use of a polycrystalline material became
evident. Most of these difficulties associated with the
fabrication of ceramic solid electrolytes can be alleviated by
using glasses. A significant breakthrough came in 1973, when
Kunze [6] prepared (largely by accident) a highly conducting
AgI/Ag_2SeO_4 glass. Subsequently, a whole family of such silver
iodide/silver oxysalt glasses was identified [7]. Thus with the
development of several high conducting glass systems ionic
conduction in glasses has attained new dimensions. Such glass
systems are called fast ion conducting glasses (FIC) and they
have very high values of ionic conductivity (of the order of
10^{-2} $(ohm-cm)^{-1}$) at room temperature. These find wide applica-
tions as solid electrolytes in various energy devices. More
than hundred FIC glasses are reported in literature almost all
of them have Li, Ag, Cu or F respectively as the migrating
species. Most of such FIC glasses are based on compositions
derived from AgI which itself is a fast ion conductor in the
crystalline form. Highest conductivity is exhibited by FIC
glasses based on silver ion migration. Only very few of the FIC
glasses are based on SiO_2 as the network former because of the
problem of silver precipitating out as metallic silver agglomera-
tes during the melting process. Large concentration of silver
ions in silica based glasses has been achieved by subjecting
the glass fibers to sodium $\rightleftharpoons$ silver ion-exchange treatment at a

well below the glass transition temperature and the effect of such an ion exchange process on electrical conductivity has been reported by Chakravorty [8].

In the following section, a brief review of the electrical properties and mechanism of electronic and ionic conduction in glasses is given.

1.1 ELECTRICAL PROPERTIES OF GLASSES

In different applications glass must serve either as an electrical insulator or a conductor and therefore, understanding of its electrical properties is important. The specific resistivities of glasses range from 10^{27} ohm-cm (calcium boro aluminate glasses) to 10^{-3} ohm-cm (amorphous metallic alloys). In between these two extremes are the oxide and chalcogenide semiconducting glasses.

1.1.1 Electronic Conduction

Great activity in devising theories for the electronic properties of disordered materials has led to understanding of some features of conduction in glassy semiconductors. The three major types of electronically conducting glasses are the following :

1.1.1.1 Chalcogenide Glasses

These glasses are those containing the Group VI (chalcoge-
nide) elements, sulfur, selenium, and tellurium, alone or in
combination with the Group V elements, phosphorus, arsenic,
antimony, and bismuth and often including other elements such as
thallium and germanium. The glasses based on cadmium arsenide
probably also belong to this category because of their similar
behavior.

Their d.c. conductivity is given by

$$\sigma = \sigma_0 \exp(-Q/kT) \tag{1.1}$$

where Q activation energy, σ_0 preexponential factor.

σ_0 and Q are temperature independent parameters. The most
striking characteristic of chalcogenide glasses is the insensiti-
vity of their conductivity to impurities. In crystalline semi-
conductors tiny concentrations of foreign atoms cause large
changes in conductivity and in the type of charge carriers,
electrons or electronholes. This is frequently attributed to the
ability of the glass to satisfy the bond requirements of the im-
purities. It may also be a result of the effects of the impurities
being swamped by defects produced by the amorphous state.

In the chalcogenide glasses conduction has been described as
occurring in an energy 'band' as in crystalline 'broad-band'

semiconductors [9]. Fritzsche [10] has proposed a hetrogenous model. In it regions in which mostly holes are localized are different from regions in which electrons are localized. He proposed that there are three kinds of electronic states: those localized in regions, channel states that extend through the material, but are excluded from certain regions, and extended states for which electrons have a finite probability of appearing anywhere in the material. A 'random-phase' model of conduction in glassy semiconductors has been proposed by Hindley [11].

The question of the species that carries the charge in chalcogenide glasses has been investigated with various electrical properties. In several different systems Hall-effect measurements indicate holes as charge carriers, whereas thermoelectric power measurements point to electrons as charge carriers.

Three mechanisms are attributed to the transport of charge carriers in chalcogenide semiconductors :

(1) Band conduction, as in crystalline materials
(2) Thermally activated hopping among localized states
(3) Polaron hopping.

The A.C. conductivity has been measured in various systems. It has been found that the variation of conductivity with frequency is given by the relation

$$\sigma(\omega) \propto \omega^n \qquad (1.2)$$

where $.7 \leq n \leq 1$.

1.1.1.2 Oxide Glasses Containing Multivalent Transition Ions

These type of glasses exhibit semiconductivity which is ascribed to its nonstoichiometry. The best known examples are the Vanadate glasses, such as $BaO.2V_2O_5$, $0.6V_2O_5.0.4Te_2O$, and various vanadium phosphate glasses. Conduction in these glasses is generally considered to arise due to 'hopping' of carriers from one strongly localized state to another. The two states are the two valence states of the transition-metal ion. Experimentally a maximum in the conductivity is found for glasses containing mixtures of ions in the two valence states, in agreement with this model. The conductivity for these glasses is given by (Mott 1968, Austin and Mott 1969)

$$\sigma = \frac{\mu_{ph}\, e^2 c(1-c)}{kTR} \, \exp(-2\alpha_\omega R) \, \exp\left(- \frac{E_H + \frac{E_0}{2}}{kT}\right) \tag{1.3}$$

where

μ_{ph} phonon frequency, c ratio of concentration of ions in lower valency to total concentration of transition metal ion, α_ω rate of decay of wave function, R average hopping distance, E_H polaron hopping energy, E_0 energy disorder.

The conduction mechanism in these glasses is diffusion like in nature and the model is based on random distribution of ions in the glass.

1.1.1.3 Glass-Metal Particulate Composites

Oxide glasses containing ultrafine metal particles exhibit semiconductivity (Chakravorty 1984). This effect has been ascribed to the tunneling of electrons from one metal grain to the next (Chakravorty et al. 1977). A theoretical model, to analyse the experimental results has been proposed. According to this, the generation of a charge carrier involves the creation of a pair of positively and negatively charged grains. The energy E_c^o required to create such a pair is given by

$$E_c^o = \frac{2 e^2}{k_1 d} \qquad (1.4)$$

where $k_1 = \epsilon [1 + \frac{d}{2s}]$

ϵ - dielectric constant of the glass

s - interparticle separation

e - electronic charge

d - metal grain diameter

If ϕ is the effective barrier height, m the electronic mass and h the Planck's constant, the mobility of charge carriers in the present system is proportional to tunnelling probability $\exp(-2xs)$ where

$$x = [\frac{8\pi^2 m \phi}{h^2}]^{1/2}$$

If $\beta(s)$ be the density of percolation paths associated with s
the conductivity is given by

$$\sigma \propto \int_0^\infty \beta(s) \, \exp[-2\times s-(c_1/2\times s kT)]\,ds \tag{1.5}$$

where

$$c_1 = \times s E_c^0 = (\frac{8\pi^2 m\theta}{h^2})^{1/2} \frac{s^2 e^2}{d\,\epsilon[1+\frac{d}{2s}]}$$

$$= \frac{2\pi e^2 \sqrt{2m\theta}}{\epsilon\,h[\frac{d}{2s}(1+\frac{d}{2s})]}$$

Under certain approximation (Abeles 1976).
Eqn. (1.5) reduces to

$$\sigma = \sigma_0 \, \exp(-2(\frac{c_1}{kT})^{1/2}) \tag{1.6}$$

Various glass metal particulate composite exhibit conductivity
variation with temperature as predicted by eqn. (1.6).

1.1.1.4 Switching Behavior

Switching and 'memory' effect in glasses have been reviewed
by Pearson and are discussed in many other papers, especially the
Journal of noncrystalline Solids, volumes 2,4 and 8 through 10.
These effects have been found in chalcogenide glasses, vanadium
phosphates, in sodium borotitanate glass and probably occur in all
semiconducting glasses.

Basically switching consists of a transition from a state
of high resistance (OFF) to one of low resistance (ON), the
transition being generated by the application of a specific
voltage named threshold voltage V_{th}. Two types of processes are
found i.e., threshold switching and memory switching. The
difference lies in the fact that in the latter, once the current
is suppressed, the state of low resistance remains. The explana-
tion given for the ON state remaining when memory switching takes
place is based on the presence of a crystalline filament which is
a consequence of the Joule heating of the amorphous material [12].

Two types of mechanisms which regulate switching have been
proposed. One is based on effects of an electronic nature [13],
the other is founded on the consequences of the current flowing
through the material [14].

1.2 IONIC CONDUCTION IN GLASSES

Ionic conductivity involves the long range migration of ionic
charge carriers through the glass under the driving force of an
applied electric field. The charge carriers will be the most
mobile ions in the glass and therefore for silicate the monovalent
cations moving in an immobile SiO_2 based matrix are the charge
carriers. The electric force on the cation serves to perturb its
random thermal motion by increasing the probability of a transition

in the direction of the applied field. This behavior can be
described by the unidirectional motion of an ion in which they
jump from one potential well to another over a barrier.
Stevels [15] and Taylor [16] calculated the probability of the
forward and backward jumps using Boltzman's distribution function
both in the absence and presence of an electrical field (E). When
a field E is applied the ion coordinates are slightly distorted
within the glass structure and the potential barrier to the ion
motion is slightly shifted. The electric field will lower the
potential barrier on the side in the direction of the field and
raise it on the otherside by an equal amount. Considering 'b'
as the distance between the two potential wells they calculated
the average drift velocity

$$V = b \, p \, \sinh \frac{Fb}{2kT} \tag{1.7}$$

where $p = a \frac{kT}{h} \exp(-W/kT)$ the probability that an ion will
move either to the right or left a-accomodation coefficient
related to the irreversibility of the jump T-Temperature,
k-Boltzman constant, h - Planck's constant, W - Maximum potential
barrier in the path of the least resistance in glass

    F = ZeE is the force on the ion
    Z - valence of the ion
    E - electric field
    e - electron charge

When the field strength is smaller then kT

$$\overline{V} = \frac{b^2 pF}{2kT}$$

The resistivity is given by

$$\log \rho = \log A + \frac{\triangle F_{DC}}{RT} \tag{1.8}$$

where $A = \text{constant} \dfrac{2h}{n e^2 \delta^2 \lambda^2}$

$\triangle F_{DC}$ - is the change in free energy for dc conduction in units of kilocalories/mole.

So a plot of $\log \rho$ vs $1/T$ results in a straight line and its slope gives the activation energy for conduction.

In deriving eqn. (1.8) it is assumed that the potential barriers are of same height. This is unlikely in case of glasses. According to the random network model the ions feel a more or less random potential energy deriving from the random network structure of glass. An ion spends most of its time at potential energy minima, but occasionally it gains energy by thermal fluctuations to pass the potential barrier which separates adjacent potential energy minima. So the measured activation energy values reflect either the average of the distribution of potential barriers or the highest potential barrier which an ion encounters.

1.2.1 Fast Ion Conducting Glasses [17]

It is well known that there are three main categories of fast ion conductors (a) α-AgI crystals, which have random distribution of cations in the anion lattice, (b) β-Alumina type crystals which have favourable structure for cation transport and (c) stabilized zirconia type crystals, which have Koch-Wagner lattice defects for anion transport. In recent years a fourth type of FICs has been found viz., amorphization or glass formation has been reported to be very useful for achieving larger conductivities than crystalline solids. FIC glasses have a high potential for use as solid electrolytes because of the following (a) a wide range of selection of composition, and thereby a wide range of property control, isotropic properties, formation of bulk materials without grain boundaries, thin film formation, feasibility of shaping and the like inherent to glasses.

Ionic species like Ag^+, Cu^+, Li^+, F^- and $O_2^=$ are reported to move fast in crystalline ion conductors. Todate however, the silver ion is the major species showing high conductivity in glassy ion conductors. While the lithium ion is attracting much attention at present.

1.2.1.1 Conduction Process in FIC Glasses

There are two theories (a) random site model and (b) weak electrolyte model.

In random site model all ions of the particular type are treated as potential carriers with a Gaussian distribution of activation energy and the mobility varies with the distribution of activation energy and thereby with the glass composition. In general the variation of carrier concentration is relatively small and thus the change in conductivity with composition is mainly controlled by the change in mobility.

In the weak electrolyte model a fraction of the total ions of that type contribute to the conduction, the remainder being associated to keep them immobile, while the mobility is independent of glass composition. Both the models are used to explain ionic conductivity in some systems of fast ion conducting glasses but inconclusive results are reported [18-19].

1.2.2 AC Electrical Properties of Oxide Glasses

The electrical response of glasses in an alternating field arises from the movement of the charged particles or dipoles restricted to distances which is the order of interatomic spacing. These require the surmounting of energy barriers. It takes a finite time for the ions to reach their final position after the field is applied. So polarization varies with time and can be represented as

$$P(t) = (P_s - P_\infty)(1 - \exp\frac{t-t_o}{\tau}) \qquad (1.9)$$

whore

τ — relaxation time

P_s — polarization at time t ∞

P_∞ — initial value of polarization

If the field alternates thurbemay be insufficient time in one half cycle for ions to reach their final positions and for the polarization to reach the final value P_s.

At very high frequencies none of the ions may move in one half fcycle and the polarization will not then exceed the instantaneous value P_∞. Continuous movement backward and forward under the action of an AC field results in a continuous absorption of energy by the material. The work done on the ions is dissipated as heat. The resultant rise in temperature decreases the relaxation time, thus increasing the number of ions which move in one half cycle. This can result in a run away situation of progressively increasing energy loss.

When a periodic electric field is applied across the sample the charge must vary with time which constitutes a charging current I_c

$$Q = CV, \quad \text{so} \quad I_c = \frac{dQ}{dt} = C\frac{dV}{dt} = i\omega CV$$

So, $I_c = \omega CV_0 \exp[(i(\omega t + \tau/2))]$ (1.10)

Thus the charging current leads the applied voltage $\pi/2$ in phase

in an ideal case. But in real cases the charging current lags
the ideal case in phase by an angle δ. The angle δ is the
loss angle and $\tan\delta$ is the loss factor. The relation between
resistivity ρ and loss factor is given by

$$\tan\delta = \frac{1}{2\pi f \epsilon' \epsilon_0 \rho}$$

where f - frequency

ϵ_0 - 8.85×10^{-14}

ϵ' - dielectric constant at the given frequency

thus

$$\sigma_{AC} = 2\pi f \epsilon_0 \epsilon' \tan\delta \qquad\qquad (1.11)$$

which is added to any DC contribution. SkSimilarly dipoles
which align in the field contribute to the AC conductivity.
Thus the electrical properties of glasses in AC field depends
on the mobile ions which give rise to the DC conductivity as
well as on the immobile ions or dipoles which constitutes a
part of the glass network.

1.2.3 Electrode Polarization

Ion transport within a glass under a DC potential eventually
leads to a build up of charge at the glass-electrode interface if

the ions are not replenished at the electrode (i.e., if the electrodes are blocking). As a result conductivity decreases with time. The reason is that the mobile cations pile up at the electrodes which results in an induced back field. The back field concentrates the potential drop in the electrode region. Since the potential across the bulk of the sample is decreased to a fraction of the applied voltage the force on the mobile ions in the bulk decreases. The back field builds up indefinitely with time resulting in a continuous decrease in glass conductivity with time.

1.3 ION EXCHANGE

If glass is placed in contact with a medium containing monovalent cations, such as a fused salt or aqueous solution, these cations can exchange with the monovalent cations in the glass matrix and interdiffuse with them into the glass matrix. An alkali silicate glass can be considered as a matrix of immobile negative groups with associated mobile cations. An exchange cation normally has a different mobility from the original ion therefore as interdiffusion proceeds one ion tends to outrun the other and an electrical potential is built up. However, accompanying this change is a potential gradient that slows down the fast ions and speeds up the slow one. To preserve charge neutrality the fluxes of the two ions should be equal and opposite and the

potential gradient ensures this inspite of the difference in the mobility of the cations [20].

1.4 STATEMENT OF THE PROBLEM

As discussed in the previous sections most of the FIC glasses contain silver as the migrating species but only very few of these glasses are based on the silicon-oxygen tetrahedral framework since it is difficult to incorporate large concentration of silver ions because of the problem of silver precipitating out as metallic agglomerates during the melting operation [21]. However, it is possible to incorporate silver ions into silicate glasses by alkali $\rightleftharpoons$ silver ion-exchange reaction at a temperature well below the glass transition temperature [22]. Under ordinary conditions of ion exchange viz., temperature around 325^0C and duration extending to 50 hours the silver rich layer is found to be only a few tens of microns thick [23]. Large concentrations of silver ions can be incorporated into SiO_2 based glasses by subjecting the glass fibers having diameters of the order of 10 microns. The effect of such an ion-exchange treatment on the electrical conductivity has been reported [Chakravorty and Srivastava] [8]. It has been found from the microstructures that the virgin glasses have a two phase structure with the dispersed phase being rich in alkali.

The microstructure reveals that these glasses after ion-exchange have interconnected silver-deficient phase and a silver-rich phase with broken interconnectivity. It has been shown that

in these ion exchanged glass fibers, an optimum combination of temperature and electric field brought about a semi-permanent reduction in resistivity and activation values respectively. Typical values of room temperature resistivity and activation energy values in this high conducting state are found to be

50 Ω cm and 0.04 eV respectively. The switching of the ion-exchanged samples to the highly conducting state under the influence of a suitable combination of temperature and electric field is believed to arise due to the formation of links between the disjointed portions of the silver rich phase. The latter being the high conducting state of the ion-exchanged sample. The forming mechanism is believed to arise due to an accelerated growth of the silver rich phase under the influence of the temperature and the electric field. The properties exhibited by these new high conducting glass systems are comparable to some of the conventional FIC glasses containing a high silver concentration than those in the above system.

It has been observed that certain $Na_2O-Bi_2O_3-B_2O_3-SiO_2$ glasses have a two phase structure with the dispersed phase being rich in alkali ions. So a silver rich phase can be induced in these glasses by subjecting them to sodium $\rightleftharpoons$ silver ion exchange treatment. Hence $Na_2O-Bi_2O_3-B_2O_3-SiO_2$ glasses with varying amount of sodium (10-30 mole %) has been chosen for the present work.

The present work has been undertaken to investigate the effect of sodium $\rightleftharpoons$ silver ion-exchange on the electrical properties of these glasses in the bulk form.

The objectives of the present thesis can be summarised as follows :

(1) To subject the glasses in the bulk form to sodium $\rightleftharpoons$ silver ion exchange treatment to get silver rich phases.

(2) To characterize the electrical properties of both the virgin and ion exchanged samples especially to see whether the ion exchanged sample in the bulk form can be switched into a high conducting state and to characterize the newly formed high conducting state.

CHAPTER II

EXPERIMENTAL TECHNIQUES

This chapter gives an account of the various aspects of preparation of glasses. Different characterization techniques employed are also included.

2.1 PREPARATION OF GLASS

All glasses investigated in the present study are prepared from reagent grade chemicals. Their compositions are given in Table 3.1. Na_2O and B_2O_3 are introduced as Na_2CO_3 and boric acid respectively and other ingredients SiO_2 and Bi_2O_3 are introduced as their respective oxides. In the present investigation, glasses are prepared by the conventional cooling technique.

2.1.1 Conventional Cooling Technique

The starting materials viz., Na_2CO_3, SiO_2, boric acid and Bi_2O_3 are mixed, in appropriated proportions, thoroughly in acetone and dried (each batch weighing around 100 gms). All these glasses have been melted in alumina crucibles using an electrically heated furnace, the temperature varying from 1000°C to 1200°C.

The glass melt is kept at the required temperature for two hours and is mechanically stirred so as to make it bubble free and homogeneous. The glasses are cast in a rectangular aluminium mould (the specimens cast has the size 5 cm x 2 cm x 0.5 cm) and subsequently annealed at 400°C for six hours. After annealing the samples are kept in a desicator.

2.2 SAMPLE PREPARATION FOR ELECTRICAL RESISTIVITY MEASUREMENTS

For electrical resistivity measurements, glass blocks are cut and all the flat surfaces are ground and polished using silicon carbide grit of different mesh sizes (100, 240, 320, 400, 600 and 800 respectively) to the approximate dimensions 10 mm x 10 mm x 1.5 mm. The crosssectional area and thickness of the specimen are measured with a micrometer (MITUTOYA MAKE). The two opposite flat surfaces, of large areas, of the specimen are coated with silver paint (NPL, New Delhi).

2.3 CONDUCTIVITY CELL

Figure 3.1 is the schematic representation of the cell used for electrical measurements. It consists of a stainless steel jacket of 300 mm length and 50 mm diameter with a cooling coil assembly at its top. The main structure of the sample holder is fitted within the jacket.
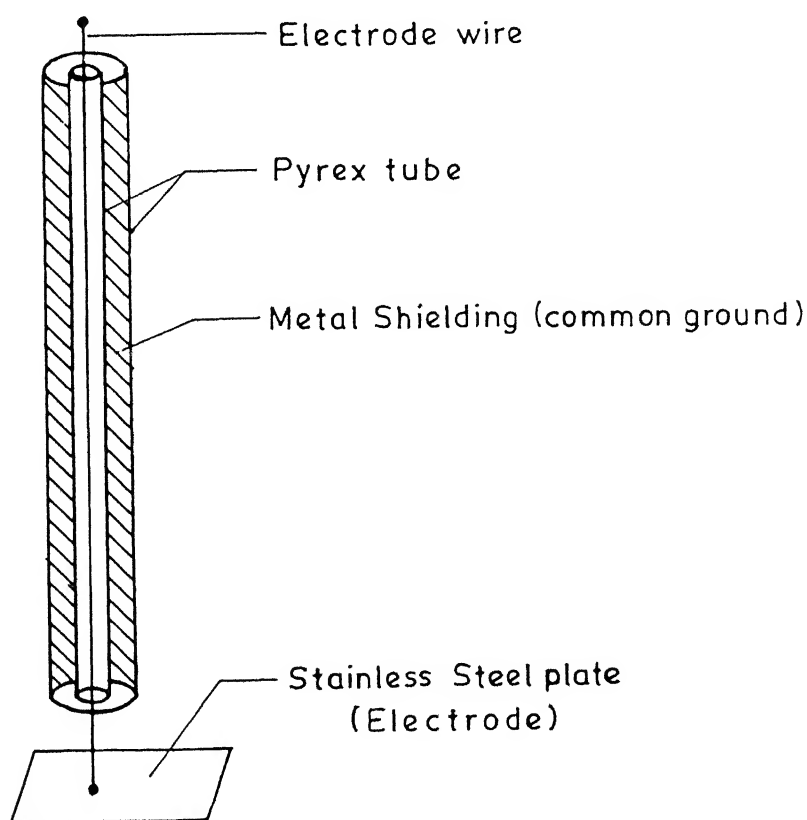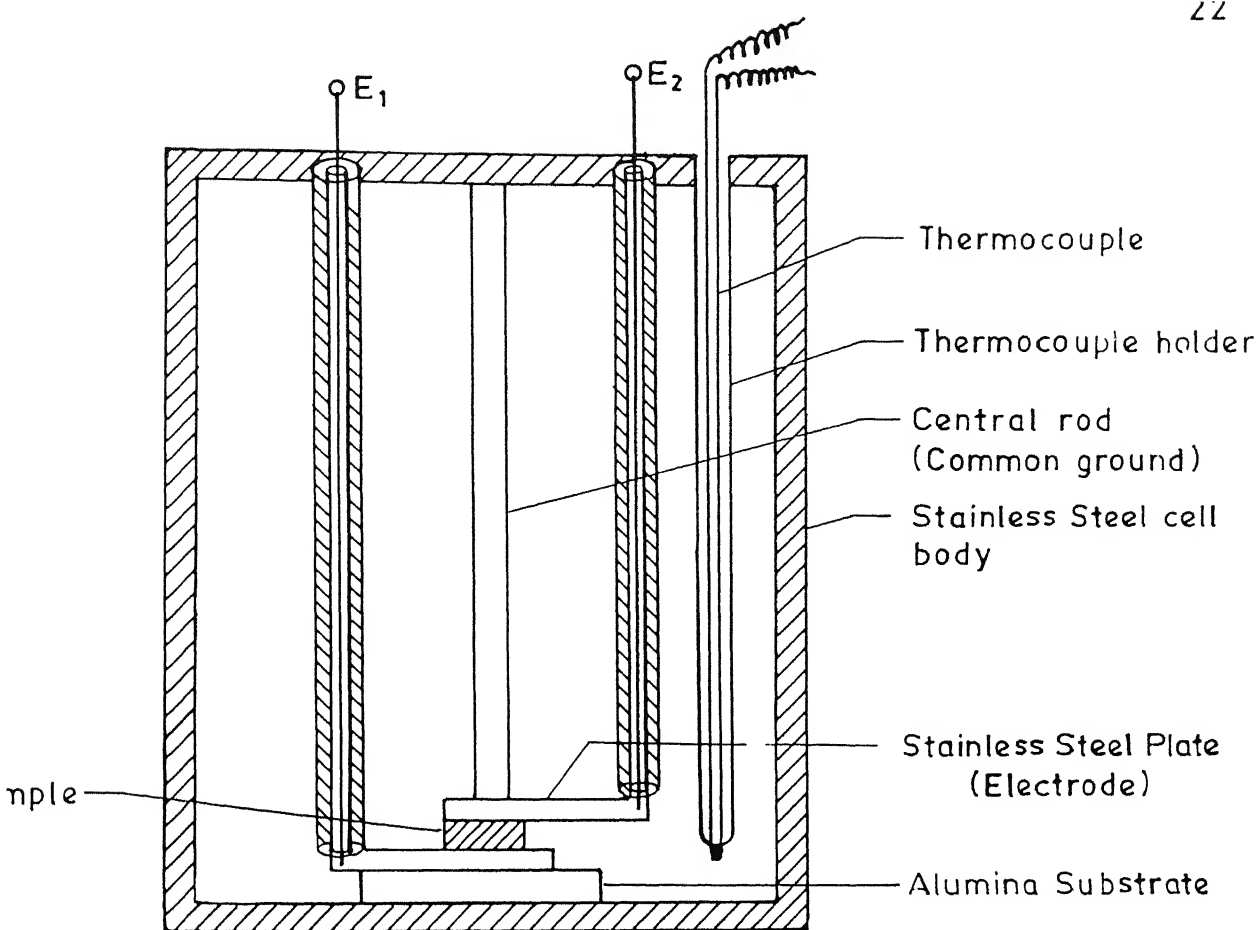
Fig. 2.1   Schematic view of the conductivity cell.

The electrodes consist of two stainless steel rods brazed to rectangular stainless steel plates so that the samples can be sandwiched between the two plates. The electrodes pass through glass tubings which have spring arrangements so that the electrodes can be moved up and down. The lower electrode is supported on an alumina substrate which itself is attached rigidly to the main structure of the cell.

The main structure of the cell consists of two stainless steel electrodes fixed to a bronze flange. The two electrodes are well shielded by metallic shiedling. The central rod in the main structure is connected to the ground. A chromel-alumel thermocouple is placed near the electrode assembly and its other end is taken out through the teflon disc fitted onto the bronze flange.

The whole assembly can be used in the temperature range from room temperature to 500°C with an accuracy of ± 1°K.

2.4 DC RESISTIVITY MEASUREMENTS

Figure 3.2 represents the schematic view of the circuit used for the measurement of current-voltage characteristics of different samples. The sample and the standard resistance are in series with a 30 volt 2 amps DC regulated power supply (APLAB model 7152). The potential drop across the standard resistance is fed to the Y-axis of an XY recorder (No. 2000 made by Digital Electronics Ltd.

India). The potential drop across the sample is fed to the
X-axis of the XY recorder. The applied voltage is varied by
the power supply and this is recorded as I-V characteristics on
the XY recorder at a given temperature.

Before each measurement the temperature of the system is
maintained constant for sufficient time (30 minutes) to attain
equilibrium by the arrangements described earlier.

2.5 AC RESISTIVITY MEASUREMENTS

The General Radio GR 1615 transformer ratio arm capacitance
bridge with GR 13136 oscillator bench and GR 1232 tuned amplifier
and null detector are used to measure capacitance and conductance
at various frequencies. At each temperature the AC resistivity is
determined by measuring capacitance and conductance at frequencies
0.1, 0.2, 0.3, 1.0, 5.0, 10.0, 20.0, 50.0 and 100 KHz respectively.
The AC resistivity is obtained from the relation

$$\rho_{AC} = \frac{A}{l} \frac{1}{G} \qquad (2.1)$$

where

        G - is conductance of the sample

        A - the area of cross-section of the silver electrodes

        l - the thickness of the specimen.

2.5.1 Complex Impedance Analysis of AC Data

The real and imaginary parts of complex impedance can be calculated by using the values of loss factor tanδ and capacitance $C(\omega)$.

The complex impedance is given by

$$Z^* = Z' - iZ'' = \frac{G}{} - i\,\frac{\omega C}{} \tag{2.2}$$

Hence, $\quad Z' = \dfrac{G}{} \tag{2.3}$

$$Z'' = \frac{\omega C}{} \tag{2.4}$$

where

$G = \omega C\,\tan\delta$ is the conductance of the sample

$\omega = 2\pi f$

f — is the frequency in Hz

C — is the capacitance.

$\tan\delta$ — is the loss factor.

The capacitance and tanδ values are measured for various frequencies at a particular temperature and the values of Z' and Z'' are calculated using equations (2.2) and (2.4).

For a fixed temperature the values of Z' and Z'' can be calculated for various frequencies from the corresponding C and

tanδ values. Complex impedance values are obtained from these data. The plot is usually a semicircle passing through the origin. The inter-section of the plot on the Z' axis is measured, which gives value of the dc resistance R_{dc}. Hence the resistivity can be calculated knowing the dimensions of the sample.

$$\rho_{dc} = \frac{A}{l} R_{dc} \tag{2.5}$$

The log ρ vs $\frac{1}{T}$ plot is a straight line and the value of activation energy can be calculated from the slope of the line.

2.6 X-RAY ANALYSIS

'Rich Seifert 2002D Isodebye flex Diffractometer' with $Cu K_\alpha$ radiation (wavelength = 0.291 mm) has been used to record the X-ray diffraction pattern of the glass samples at a scanning speed of 3° per minute. The glass samples are ground thoroughly to very fine powder in an agatemotar and then sieved out in the range of -14 mesh to -20 mesh (particle size   10 μm) and these fine powders are analysed by powder diffraction method.

2.7 SAMPLE PREPARATION FOR ION-EXCHANGE

The glass samples are polished to the dimensions of about 2 mm x 2 mm x 2m by silicon carbide grits of various mesh sizes (100, 200, 320, 400, 600 and 800) respectively. Then the sample is washed in acetone, dried and kept in a pyrex boat containing

molten silver nitrate at 325 °C in an electrically heated furnace
for 50 hours. After the ion-exchange treatment the sample is
taken out washed and boiled in water for a couple of hours to
remove any silver nitrate sticking on the sample surfaces.
Finally it is washed in acetone, dried and kept in a desicator.

For electrical resistivity measurement silver paint is
applied on two opposite faces after measuring the exact cross-
sectional area and thickness of the sample with a micrometer
(MAKE).

The **electrical resistivity** measurements/complex impedance
analysis of AC data are done exactly in the same manner as for
virgin glasses.

2.8 POLARIZATION EMF CURVES

Wagner's asymmetric **polarization cell technique** [24] has
been used in this investigation **to determine the** conductivity
of glassy electrolyte **in the high** conducting **state. Silver
paint served as the** reversible electrode **whereas graphite paint**
(Polaron **Equipment Ltd.,** England) **served as the blocking electrode**

The Cell Ag/High conducting glass system/$c^{(+)}$ is clamped in
the sample holder. The temperature of the furnace **is raised and
maintained at a constant temperature for 30 minutes before polari-
zing the cell.** Small polarising voltages **are** applied **by a** potentio
stat and the polarising current is monitored. **For each of the**

voltages the steady state current is recorded, in each case until there is an abrupt rise of current.

2.9 BLOCKING ELECTRODE EXPERIMENT

On the two opposite surfaces of the high conducting glass specimen graphite paint is applied which serve as blocking electrodes. The cell C/glass/C is sandwiched between the two stainless steel electrodes. The temperature of the furnace is raised and maintained at a constant level for 30 minutes. A potential of one volt is applied across the sample. The conductivity of the sample in the high conducting state is measured as a function of time. This experiment is done at various temperatures.

Conductivity as a function of time is calculated from the volt current characteristics at various time. Fig. 3.2 gives the circuit diagram. Here the same amount of current flows through the standard resistance in series and through the sample. As time goes due to polarization the resistance of the sample increases so the voltage across the sample increases and the current through the sample decreases with time. And this variation is recorded in an X-Y recorder. Fig. 3.24 gives such a plot. Each point in the curve from the break is timed. The resistance of the sample corresponding to each point is calculated and from this the conductivities at various time are estimated. Finally the conductivity is plotted against time Fig. 3.25.

CHAPTER III

RESULTS AND DISCUSSION

The virgin glass specimens which have been investigated are referred to as glass system G. Table 3.1 gives the composition of these glass systems. The ion-exchanged glass samples are being referred to as IG glass system and the high conducting glass samples are referred to as HIG glass systems.

3.1 ION-EXCHANGE

Samples for ion-exchange treatment are prepared as given in Section 2.7. These samples of each composition have been ion-exchanged in a pyrex boat containing molten $AgNO_3$ at 325°C for 50 hours. After ion exchange the thickness of the silver rich layer has been calculated from the sodium$\rightleftharpoons$silver inter-diffusion data (Chakravorty 1976 [25]) published earlier. The morphology of the ion exchanged sample can be represented schematically as shown in Fig. 3.0. Table 3.2 gives the thickness of the silver rich layer for each composition and each temperature of treatment respectively.

3.2 X-RAY ANALYSIS

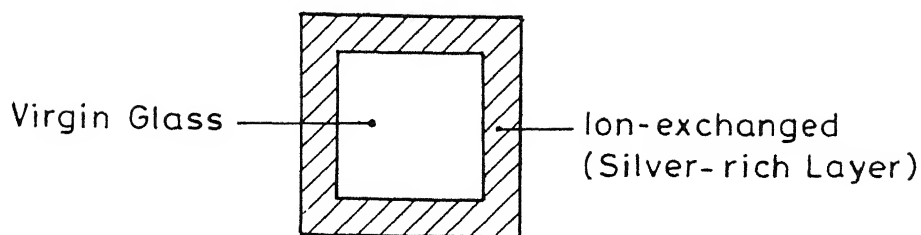A broad peak which is characteristic of an amorphous material is found in each case.

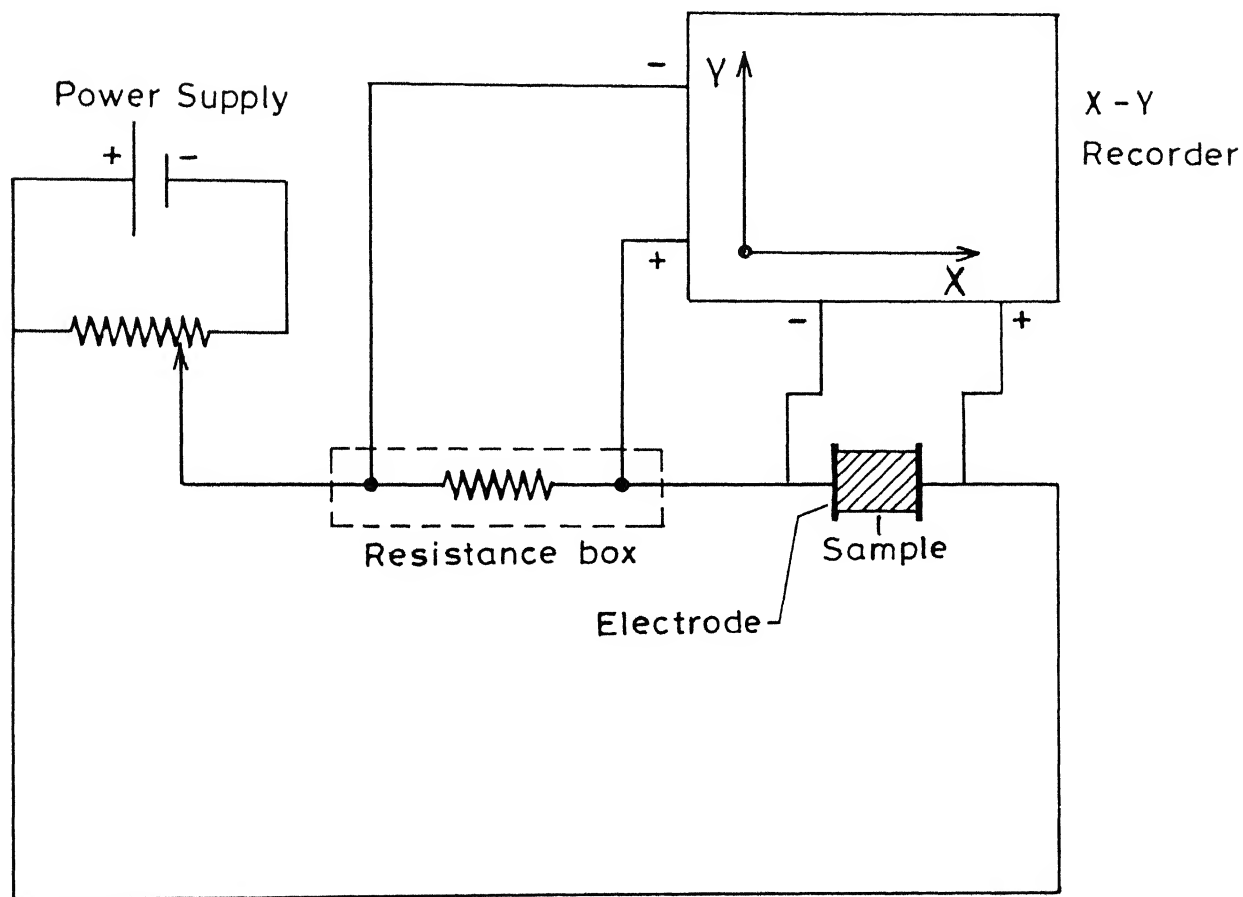Fig. 3.1 Schematic representation of the morphology of ion-exchanged sample.

Fig. 3.2 Schematic circuit diagram for DC Resistivity measurements.

S. No.	Glass	Na$_2$O	Mole %		
		Na$_2$O	SiO$_2$	B$_2$O$_3$	Al$_2$O$_3$
	G$_1$	10	64	18	8
	G$_2$	23	54	15	8
	G$_3$	30	52	10	8

able 3.2 Thickness of the silver rich layers in ion-exchanged samples

S. No.	Glass	D_{Na} (cm^2/sec)	D_{Ag} (cm^2/sec)	Thickness of the silver rich layer (cms)
	IG$_1$ (IE at 325°C)	3.2x10^{-12}	3.2x10^{-12}	7.6x10^{-4}
	IG$_1$ (IE at 350°C)	4.5x10^{-12}	4.5x10^{-12}	9.1x10^{-4}
	IG$_2$ (IE at 325°C)	3.3x10^{-12}	6.6x10^{-12}	7.7x10^{-4}
	IG$_2$ (IE at 350°C)	5.2x10^{-11}	2.1x10^{-10}	3x10^{-3}
	IG$_3$ (IE at 325°C)	3.3x10^{-12}	6.6x10^{-12}	7.7x10^{-4}
	IG$_3$ (IE at 350°C)	5.2x10^{-11}	2.1x10^{-10}	3.0x10^{-4}

3.3 ELECTRICAL MEASUREMENTS

AC and DC resistivity measurements for the glass systems
have been carried out as discussed in Sections 2.4 and 2.5. I-V
plots are obtained on X-Y recorder by the circuit described in
Section 2.4. The slopes of these curves give DC resistance of
the sample.

3.3.1 AC Measurements and Complex Impedance Analysis

AC measurements yield the values for conductance (G) and
capacitance (C) as a function of frequency (f). The frequency
has been varied from 200 Hz to 100 KHz. Impedance analysis have
been carried out for all these glasses at various temperatures.
The real (Z') and imaginary (Z") parts of impedance are calculated
by eqns. (3.1) and (3.2)

$$Z' = \frac{G}{G^2 + \omega^2 C^2} \qquad\qquad (3.1)$$

$$Z" = \frac{\omega C}{G^2 + \omega^2 C^2} \qquad\qquad (3.2)$$

Various points in the Z' - Z" plane are found to lie on the arc
of a semicircle passing through the origin, the centre lying
on the X-axis. The intersection of this arc on the real (Z')
axis other than the point of intersection at the origin yields the
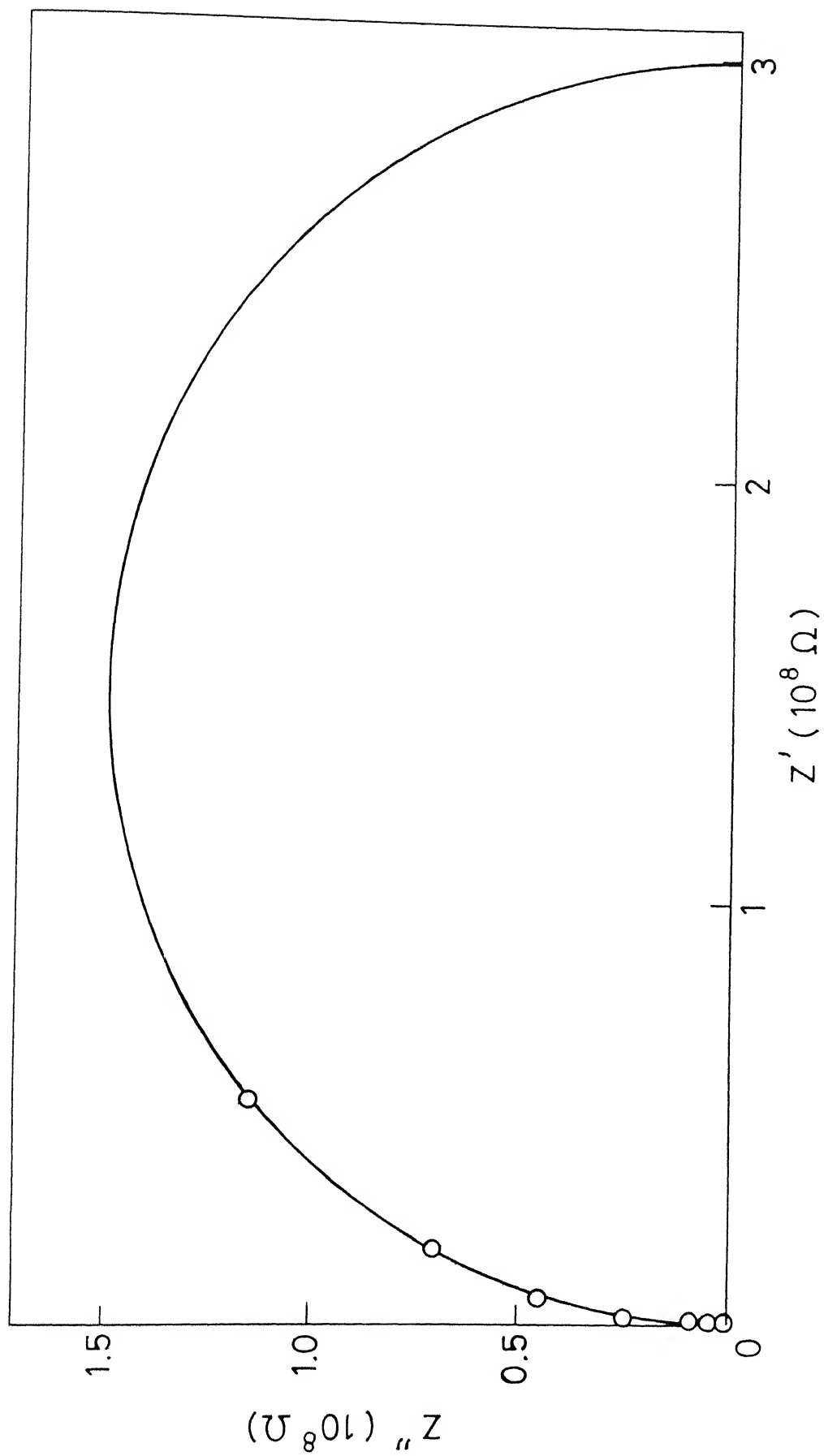
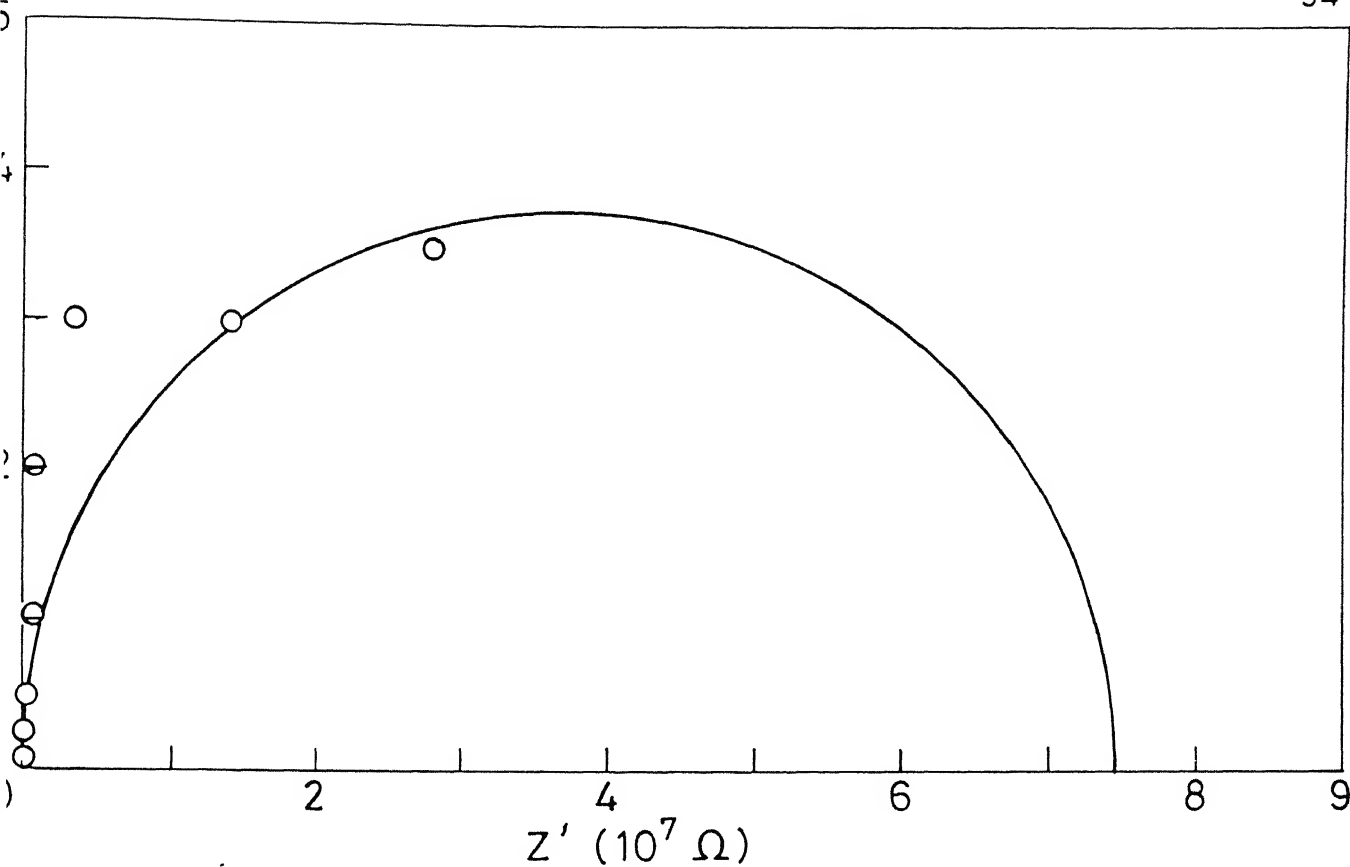Fig. 3.3 Complex impedance plot for glass system G_1 (T = 100°C)

Fig. 3.4 Complex impedance plot for glass system IG_1 .
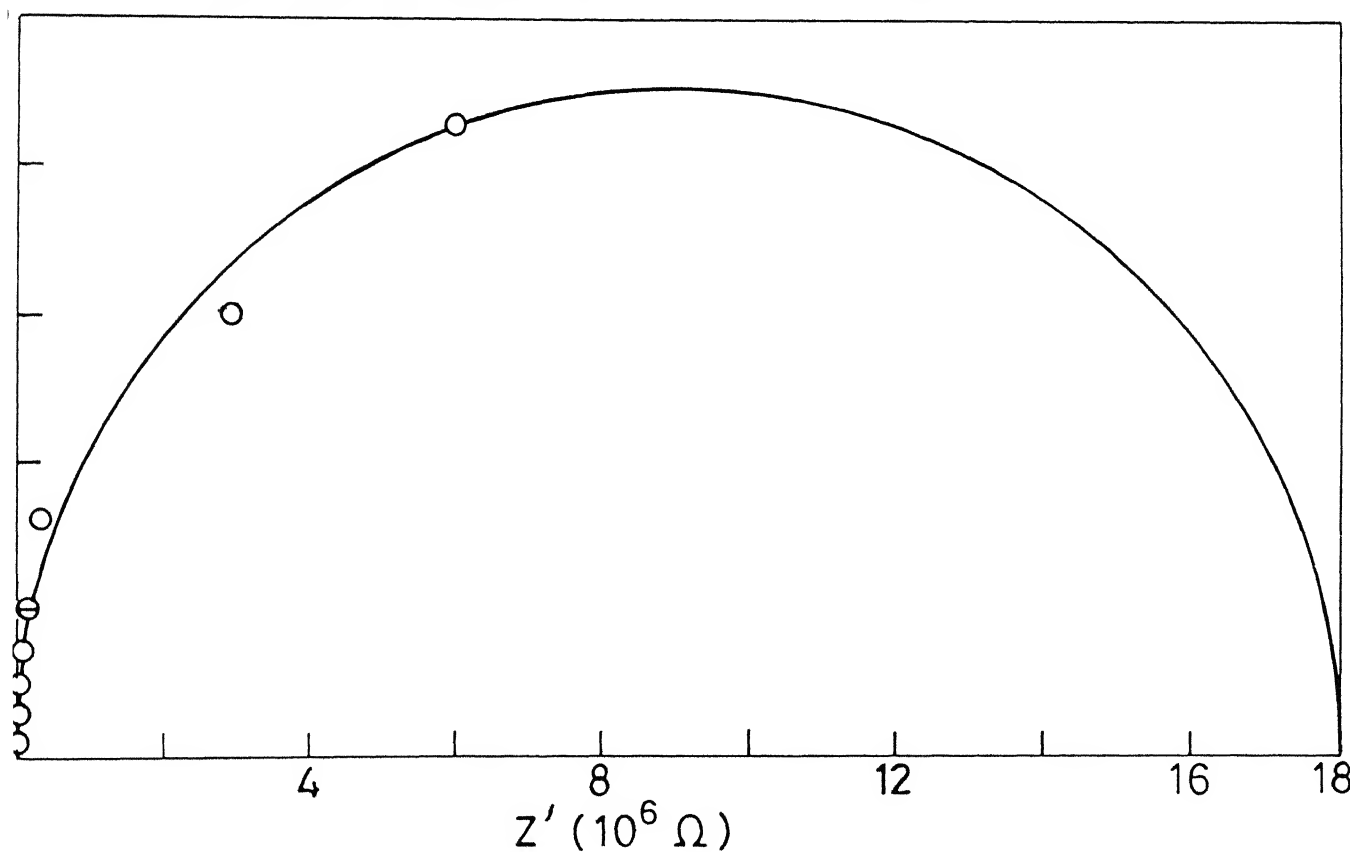Ion exchanged at $350^{\circ}C$ ($T = 68^{\circ}C$)

Fig. 3.5 Complex impedance plot for glass system G_2 ($T = 153^{\circ}C$)
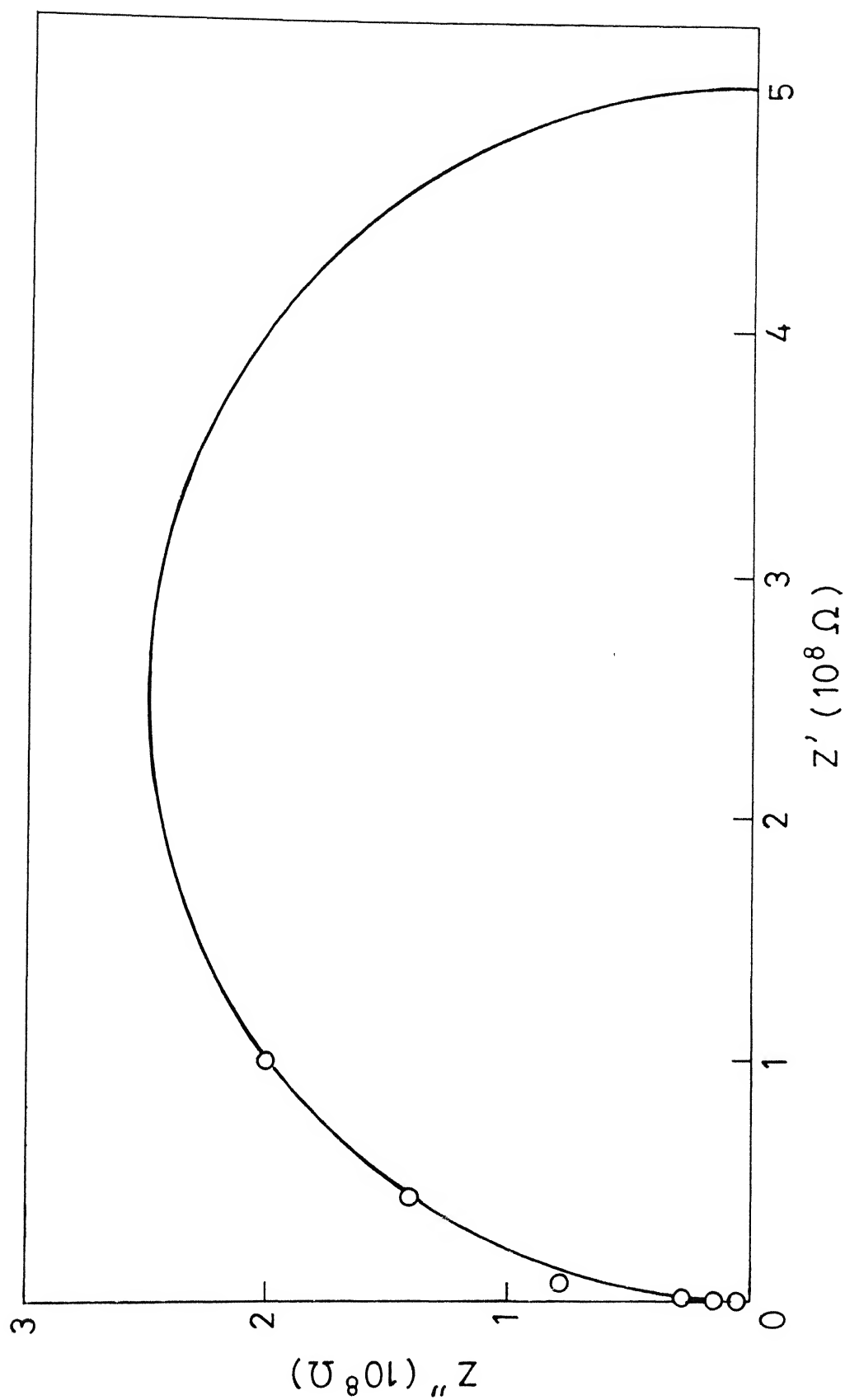
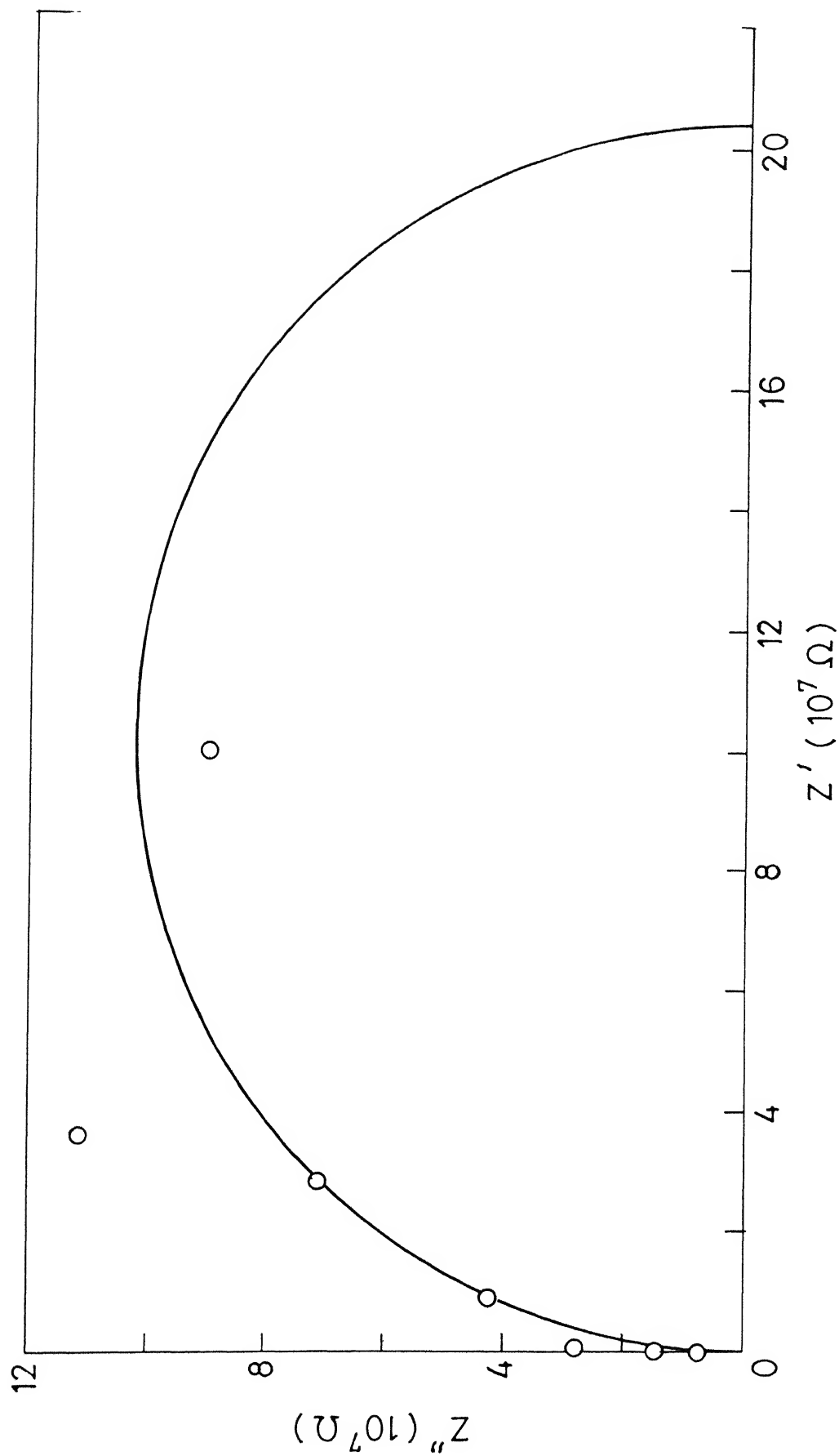Fig. 3.6 Complex impedance plot for glass system IG_2 Ionexchanged at 325°C (T = 46°C)

Fig. 3.7 Complex impedance plot for glass system IG_2 Ionexchanged at $350°C$ ($T = 60°C$)
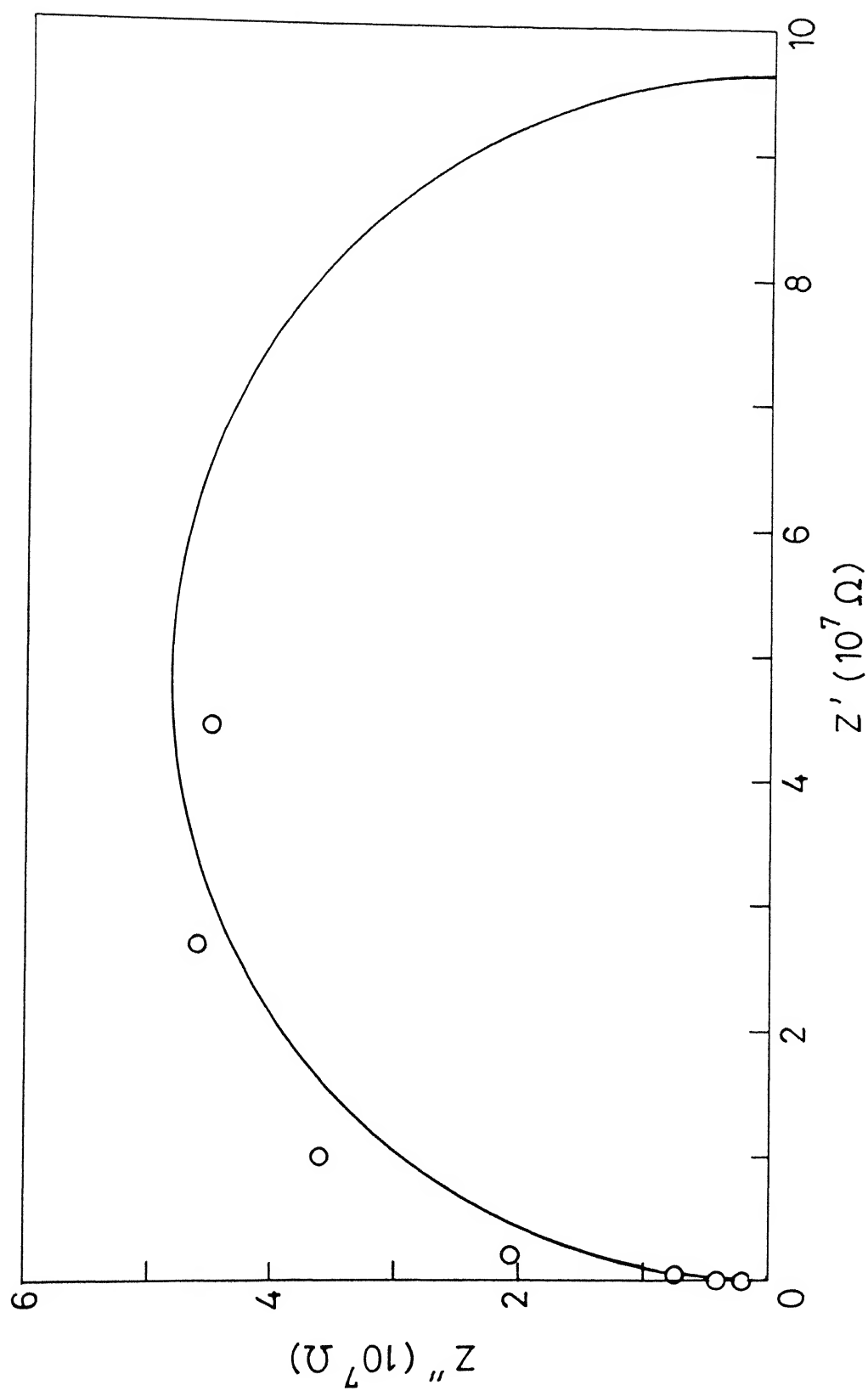
Fig. 3.8 Complex impedance plot for glass system G_3 (T = 46°C)
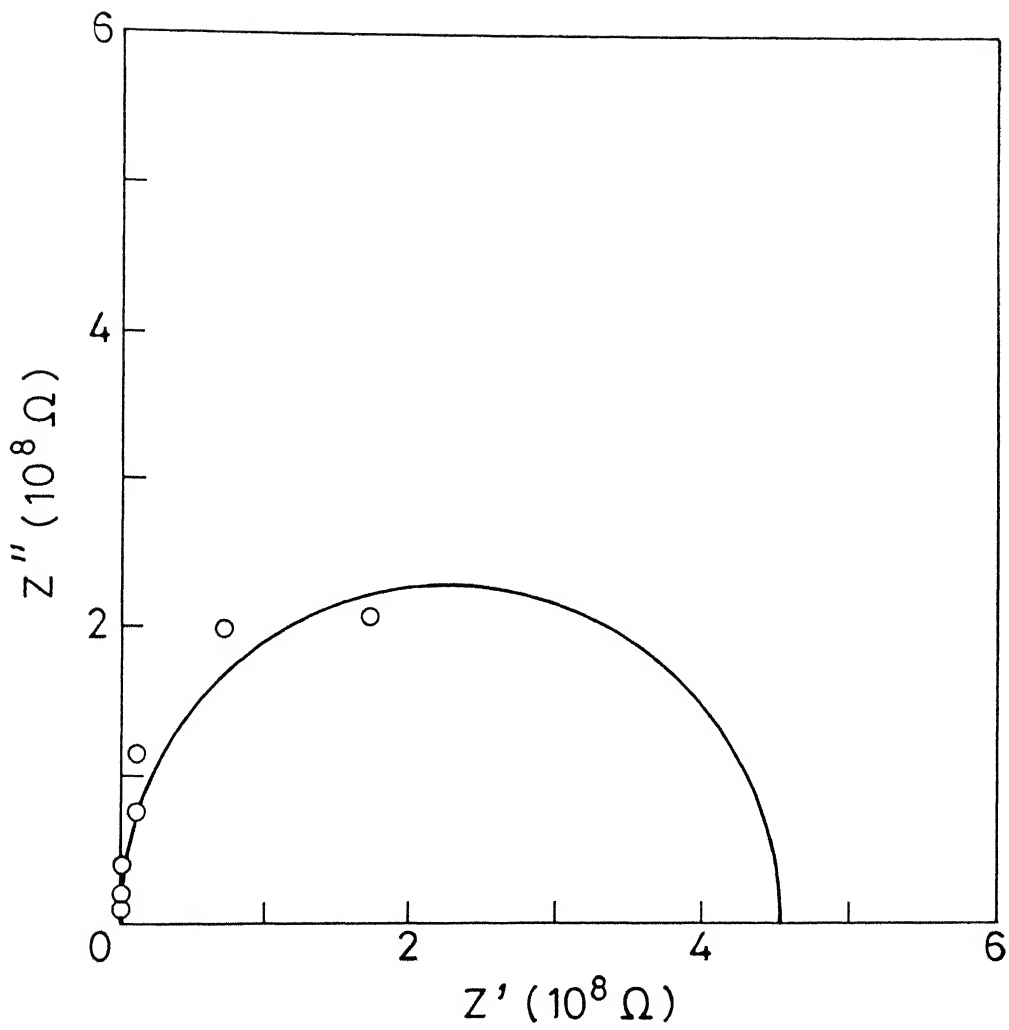
Fig. 3.9 Complex impedence plot for glass system
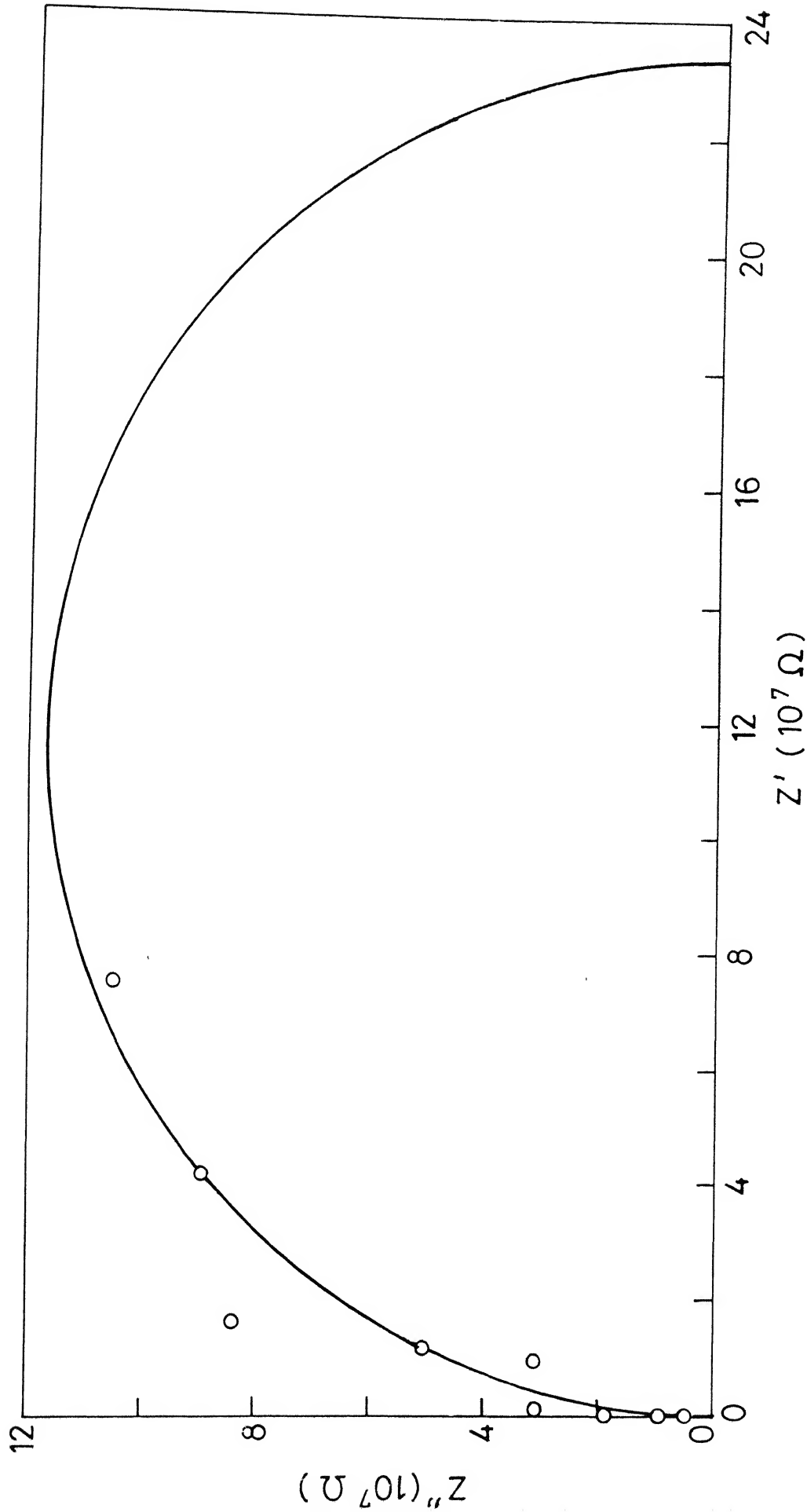IG$_3$ Ionexchanged at 325°C (T = 46°C)

Fig. 3.10 Complex impedance plot for glass system IG_3 Ionexchanged at 350°C ($T_c = 46°C$)

DC resistance R_{dc} of the sample. Figs. 3.3 to 3.10 are typical
Z" - Z' plots for the different virgin and ion-exchanged glass
systems.

3.4 TEMPERATURE DEPENDENCE OF RESISTIVITY

Resistivity of various glass samples has been calculated
from the complex impedance plot for various temperatures in the
range 20°C to 320°C for the virgin glass systems and ion-exchange
glass systems.

It has been found that ion-exchanged glass (IG) samples
invariably show a sudden surge of current when the applied
electric field E exceeds a critical value E_C. The value of the
critical field E_c is dependent upon the temperature (T_c) for a
given glass composition. Thus an optimum combination of electric
field and temperature brings about a permanent change in the
resistivity of these glass systems. The newly attained state
has resistivities many orders of magnitude lower than that of
the ion-exchanged glass system. Once the ion-exchanged glass
system attains this high conducting state it is being referred
to as HIG glass system.

The typical switching behaviour (I-V plots) of an ion-
exchanged glass systems (IG) to high conducting glass (HIG) syste
has been shown in Figs. 3.11 to 3.16. In these figures both IG
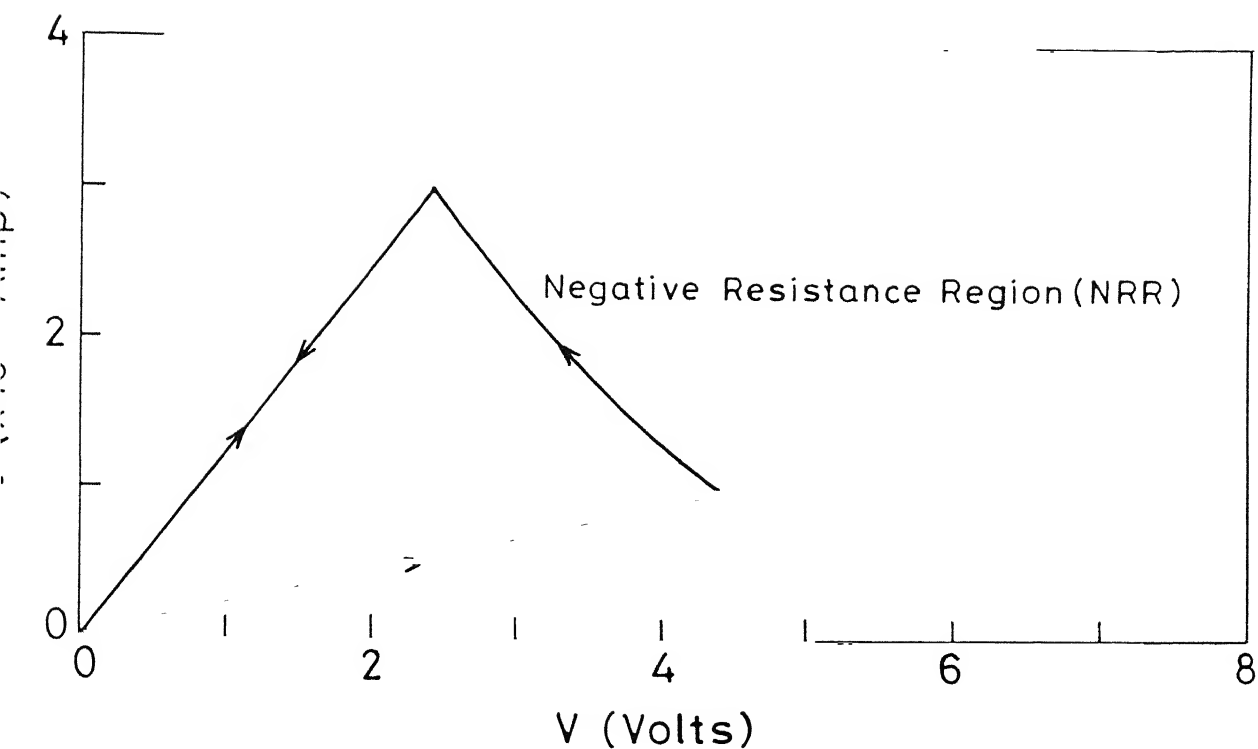state and HIG state are shown. These plots are characterized by

Fig. 3.11 Switching of glass system IG_1 ionexchanged at 350°C to HIG_1 glass system ($T_C = 360$°C)

Fig. 3.12 Switching of glass system IG_1 ionexchanged at 325°C to HIG_1 glass system ($T_C = 377$°C)

ig. 3.13 Switching of glass system IG_2 ionexchaged at $350°C$ to HIG_2 glass system ($T_C = 231°C$)

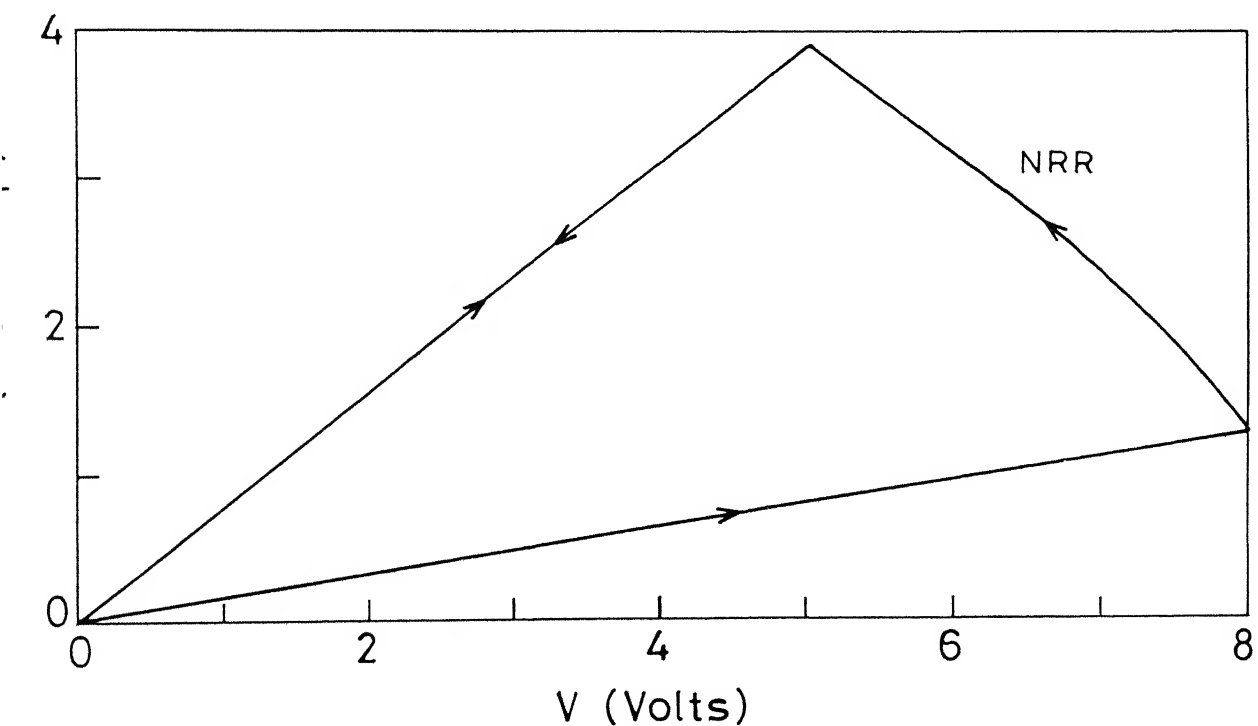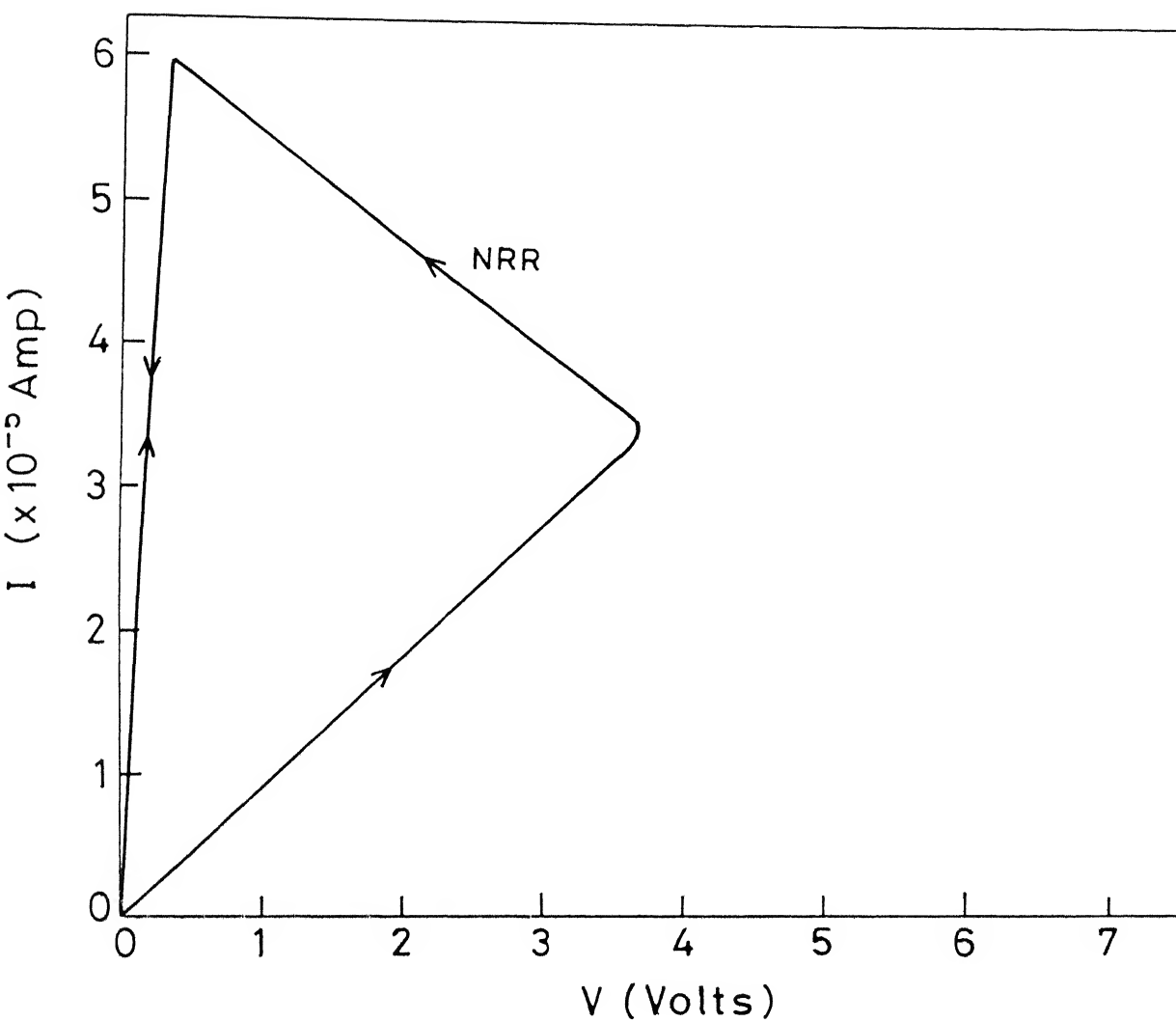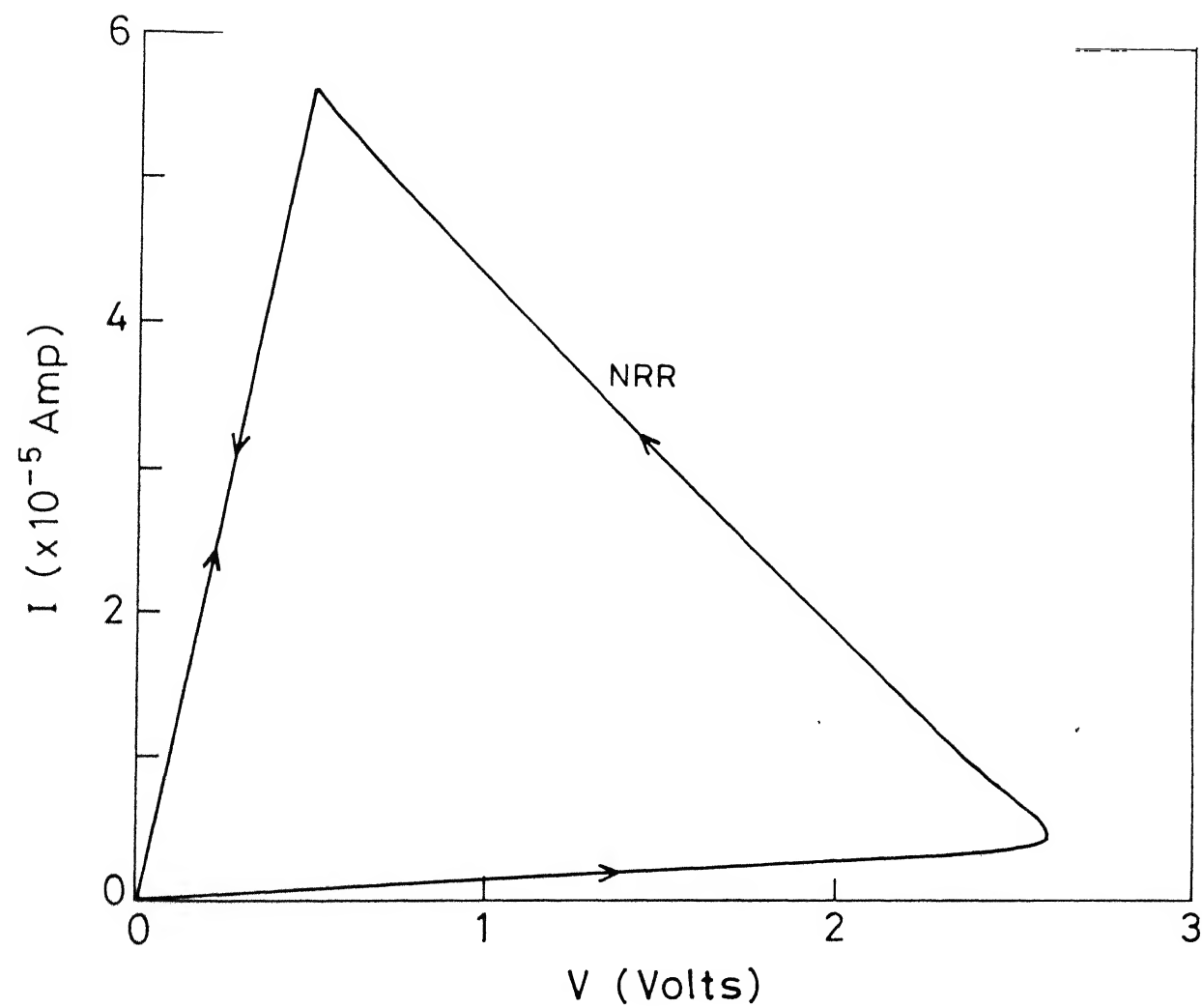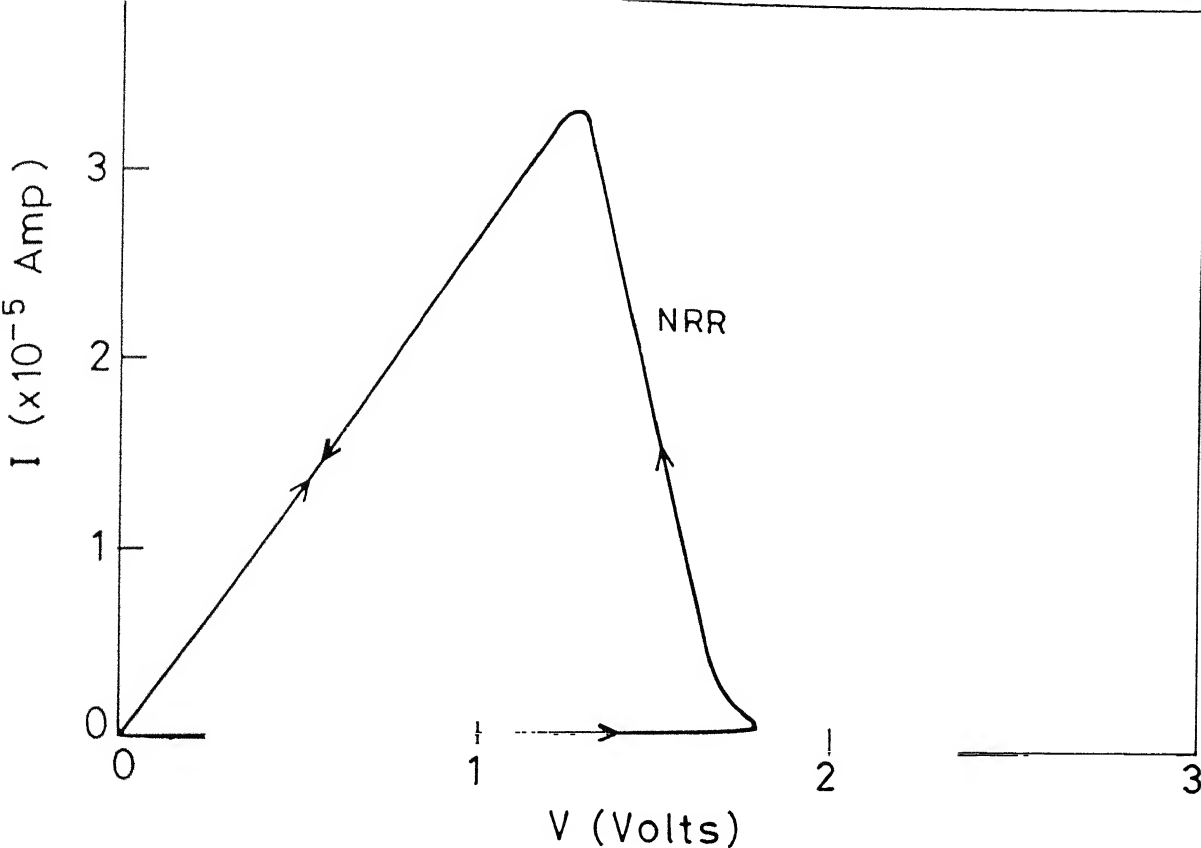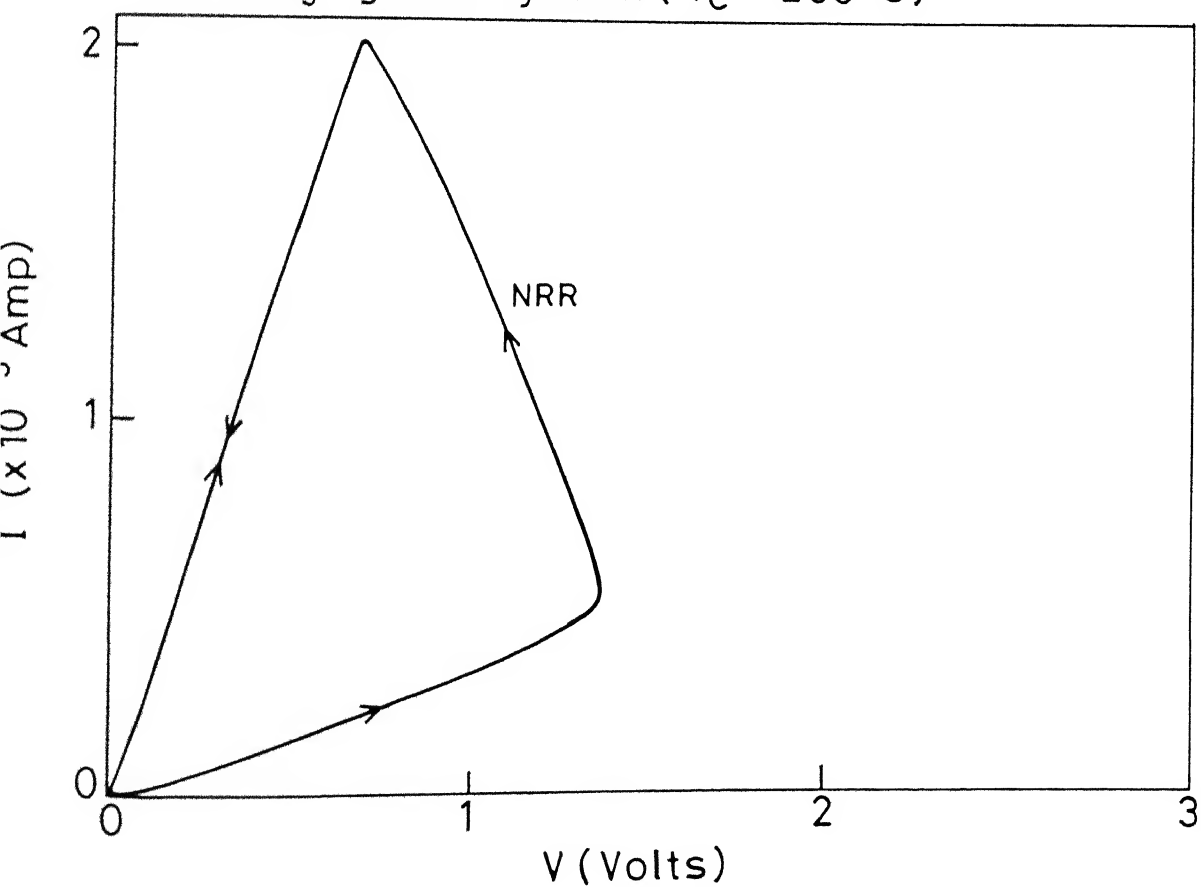Fig. 3.14 Switching of glass system IG_2 ionexchanged at $325°C$ to HIG_2 glass system ($T_C = 285°C$)

g. 3.15 Switching of IG$_3$ glass system ionexchanged at 325°C to HIG$_3$ glass system (T$_C$ = 288°C)

g. 3.16 Switching of glass system IG$_3$ ionexchanged at 350°C

negative resistance region shown by arrows in these figures.
High conducting state is stable and HIG glass systems are new
materials characterised by high conductivity. Variation of
threshold field with temperature for IG glass systems are shown
in Fig. 3.17.

Figures 3.18 to 3.20 show the variation of log ρ with 1/T
for virgin (G) ion-exchanged (IG) and high conducting (HIG) glas
system. Figs. 3.21 and 3.22 show log ρ vs 1/T for the glass
system G and glass system IG respectively.

The temperature dependance of resistivity in each case bein
assumed to follow the relationship

$$\rho = \rho_o \exp(\frac{Q}{kT})$$

where ρ - resistivity of the sample
          ρ_o - pre-exponential factor
          Q - activation energy for conduction
          k - Boltzman constant
          T - temperature

Tables 3.3 to 3.7 give the values of preexponential factor (ρ_o)
and activation energy Q for the glass system G, glass system IG
and glass system HIG respectively.

Fig. 3.17 Temperature variation of critical electric field (E_C) for glass system IG.

Fig. 3.18 Temperature variation of DC resistivity for glass systems G_1, IG_1 and HIG_1.

Fig. 3.19 Temperature variation of DC resistivity for G_2, IG_2 and HIG_2 glass systems.

Fig. 3.20 Temperature variation of DC resistivity for G_3, IG_3 and HIG_3 glass systems.

Fig. 3.21 Temperature variation of DC resistivity for G_1, G_2 and G_3 glass systems.

The following appear within the figure:

- y-axis: $\log \rho \ (\Omega \ cm)$
- x-axis: $1000/T \ (K^{-1})$

Legend:

○ G_1
$Q = 0.79 \, eV$, $\rho_o = 3.2$

□ G_2
$Q = 0.63 \, eV$, $\rho_o = 1.58$

△ G_3
$Q = 0.57 \, eV$, $\rho_o = 4.03$

Fig. 3.22 Temperature variation of DC resistivity for IG_1, IG_2 and IG_3 glass systems.

Table 3.3　Activation energy and preexponential factor for the glass system G

Sl. No.	Glass	$Q \pm dQ$ (eV)	$\rho_0 \pm d\rho_0$ (ohm cm K^{-1})
1	G_1	0.79 ± 0.13	3.2 ± 3.5
2	G_2	0.63 ± 0.12	1.58 ± 2.1
3	G_3	0.57 ± 0.13	4.03 ± 3.1

Table 3.4　Activation energy and preexponential factors for the glass system IG (ion-exchanged at 325°C)

Sl. No.	Glass	$Q \pm dQ$ (eV)	$\rho_0 \pm d\rho_0$ (ohm cm K^{-1})
1	IG_1	0.63 ± 0.13	2.1 ± 2.0
2	IG_2	0.56 ± 0.08	4.4 ± 4.7
3	IG_3	0.44 ± 0.10	11.4 ± 11.0

Table 3.5 Activation energy and preexponential factor for the glass system IG [Ion exchanged at 350°C]

Sl.No.	Glass	$Q \pm dQ$ (eV)	$\rho_o \pm d\rho_o$ (ohm cm K^{-1})
1	IG$_1$	0.62 ± 0.13	$3.3 \times 10^{-2} \pm 3.0 \times 10^{-2}$
2	IG$_2$	0.56 ± 0.08	0.39 ± 0.4
3	IG$_3$	0.43 ± 0.1	5.07 ± 6.0

Table 3.6 Activation energy and preexponential factors for the glass system HIG (ion exchanged at 325°C and switched to the high conducting state)

Sl.No.	Glass	$Q \pm dQ$ (eV)	$\rho_o \pm d\rho_o$ (ohm cm K^{-1})
1	HIG$_2$	$.005 \pm .002$	39.8 ± 86.3
2	HIG$_3$	$-(.005) \pm .003$	39.8 ± 2.39

Table 3.7 Activation energy and preexponential factors for the glass system HIG (Ion exchanged at 350°C and switched to the high conducting state

Sl.No.	Glass	$Q \pm dQ$ (eV)	$\rho_o \pm d\rho_o$ (ohm cm K^{-1})
1	HIG$_1$	-0.006 ± 0.003	4.35 ± 0.26
2	HIG$_2$	0.002 ± 0.0006	0.74 ± 0.15
3	HIG$_3$	-0.002 ± 0.0009	6.90 ± 0.42

3.4.1 Polarization Method

3.4.1.1 Wagner's Asymmetric Polarization Technique

The Wagner's asymmetric polarization technique and the theory behind it has already been discussed in Sections 2.8. a 1.2.3 respectively.

The polarization cell of the form Ag/glass/C(+) in which metallic silver and graphite act as reversible and blocking electrodes respectively has been studied. Here the glass sam is the high conducting HIG glass system. Small voltages are app and steady state currents is observed. At a particular temper current initially increases with applied voltage and attains a plateau where the steady state current is independent of appli voltage. The current voltage curves are illustrated in Fig. 3 for various temperatures.

3.4.1.2 Blocking Electrode Method

Experimental technique and theory are discussed in Section 2.9 and 1.2.3 respectively. The cell C/glass/C is sandwiched between the two stainless steel electrodes. The graphite paint applied on the two opposite sides of the sample acts as two blocking electrodes. Here the sample is the one which is in th high conducting state, i.e., HIG glass system.

A potential of 1 volt is applied and the conductivity of t

sample is measured as a function of time. This experiment is done at various temperatures. The conductivity time curves are plotted in Fig. 3.25 for various temperatures.

It is is found that at a particular temperature the conductivity decreases with time. The initial decrease in conductivity is more abrupt, as time goes the steep fall in conductivity curve take a plateauv like form. The results are shown in Fig. 3.25.

3.5 DISCUSSION

Activation energy for conduction and the resistivity is found to be decreasing with increasing amount of Na_2O. It is because an increase in the amount of Na_2O content leads to an enhancement of the non-bridging oxygen ions and hence a lowering of the rigidity of the glass network (Rawson 1984 [25]). In G glass systems the conduction is due to the sodium ion migration so the conductivity increases with increasing amount of sodium ions.

Ion-exchanged glass system shows a decrease in resistivity and activation energy. This has been explained on the basis of ionic radii of sodium ion and silver ion respectively (Chakraverty [26]). It has been shown (Stevels [27]) that the activation barrier to ionic transport in oxide glasses is comprised of two parts, electrostatic and mechanical. If the glass
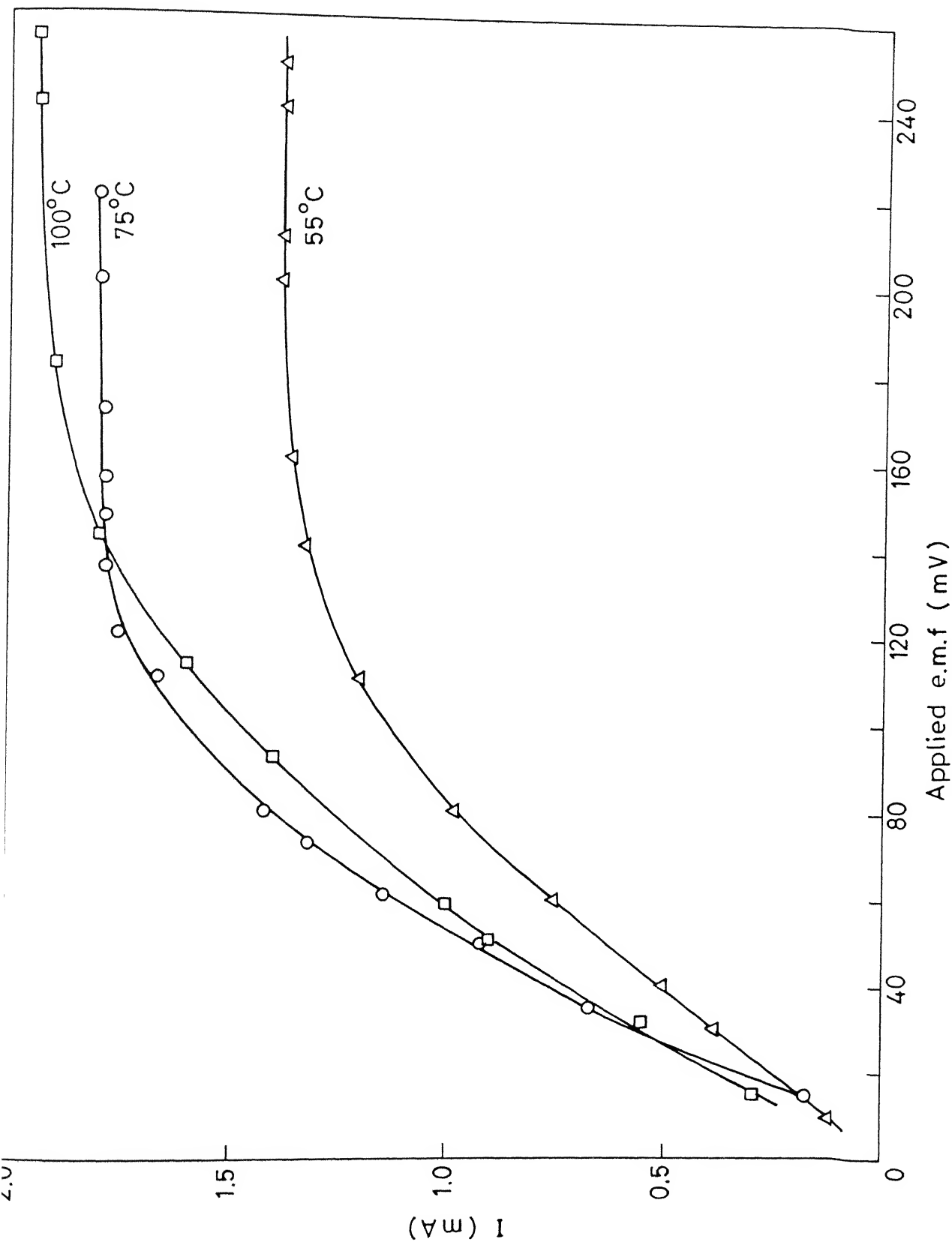
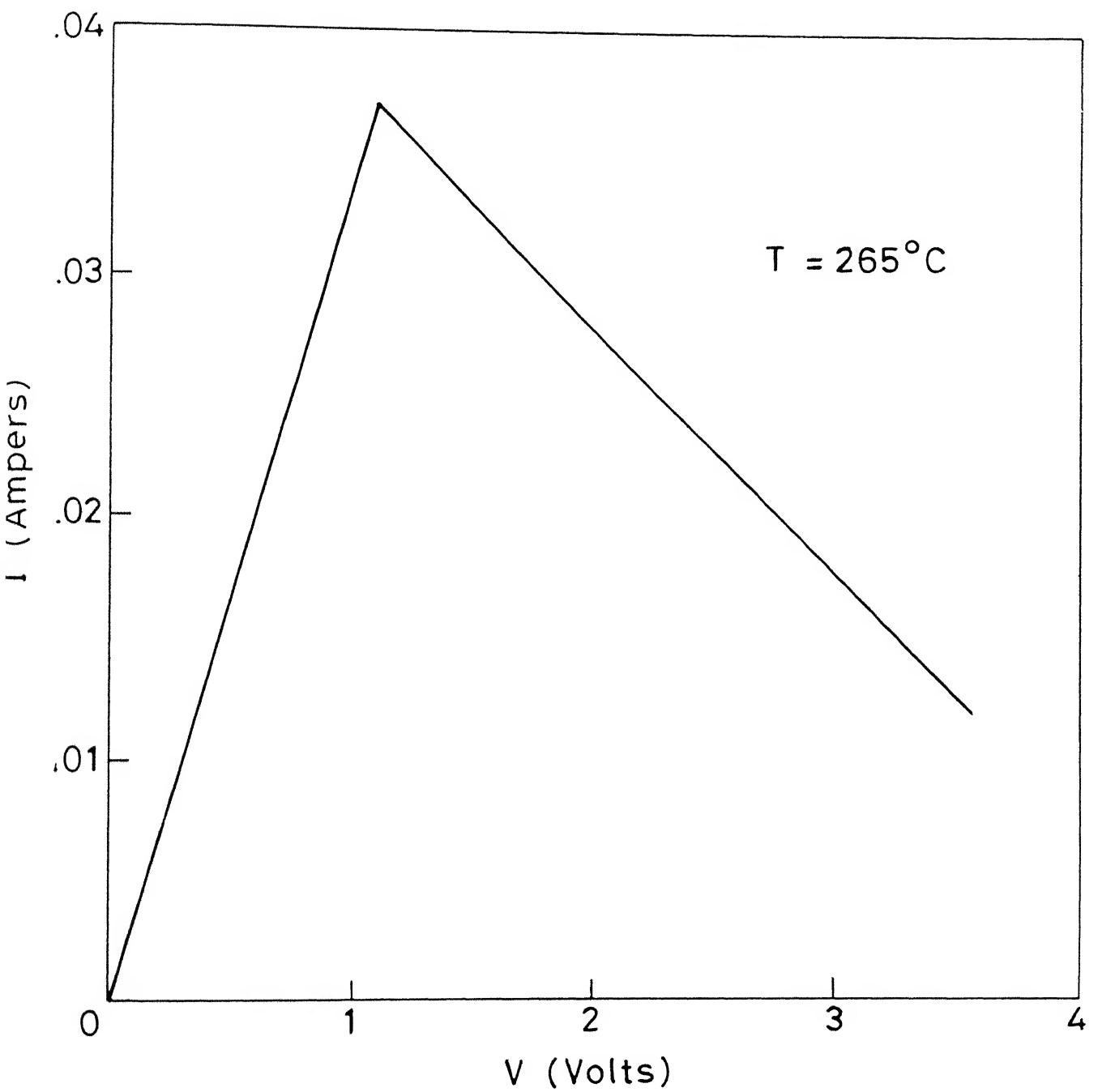Fig. 3.23 Steady state current voltage curves for the polarization cell $Ag|HIG_2|C^+$

Fig. 3.24 Current Voltage charecteristics for C|HIG₃|C cell.

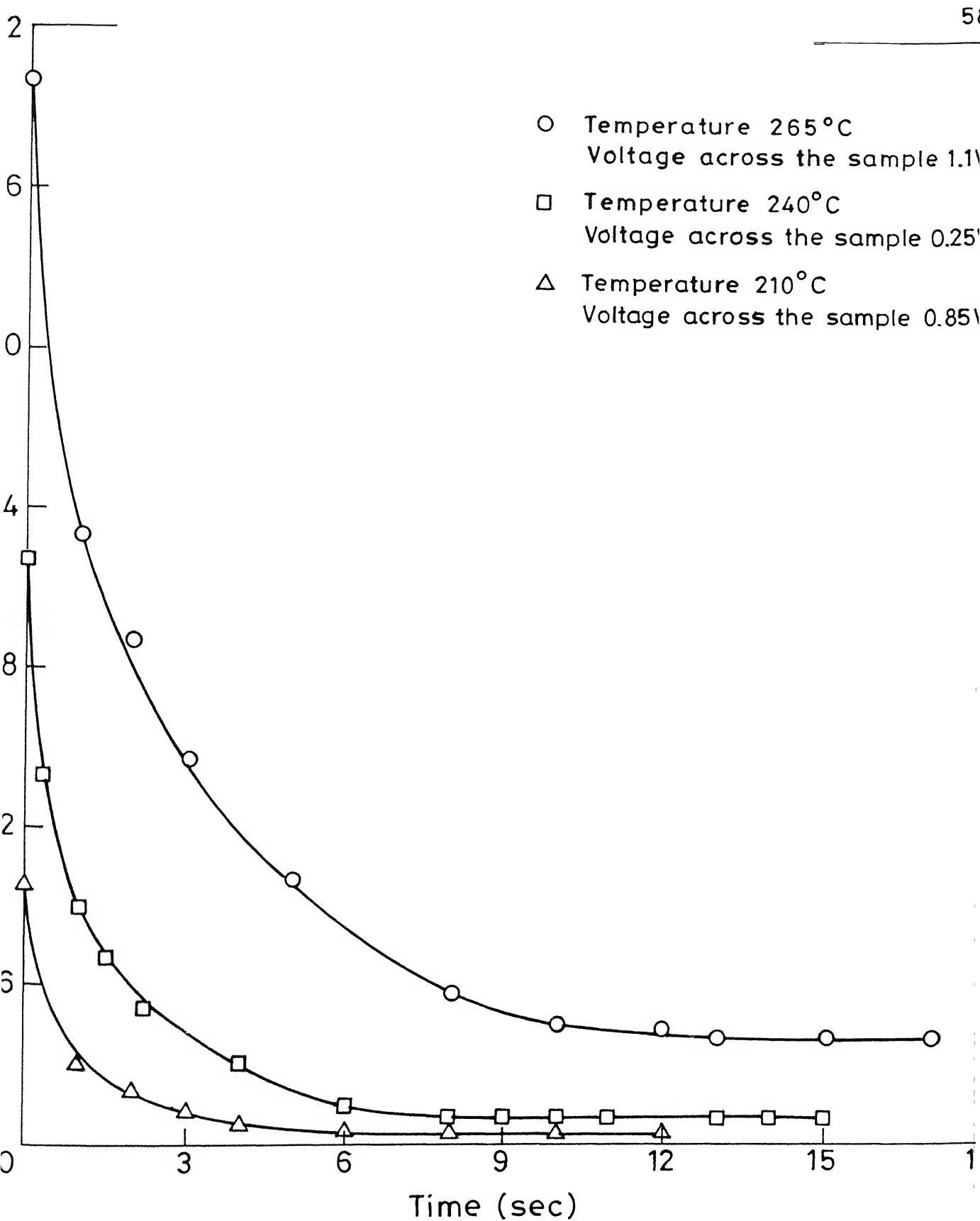Fig. 3.25 Conductivity as a function of time for $52\,SiO_2 \cdot$
$30\,Na_2O \cdot 10\,B_2O_3 \cdot 8\,Bi_2O_3$ glass ionexchanged ($Ag \rightleftarrows Na$)
at 350°C for 48 hrs and switched, at various temp-
eratures and voltages.

system is sufficiently open which is the case when enough
alkali ions are present (valid in our glass system) the contri-
bution due to elastic distortion of the glass structure (mecha-
nical energy) to the activation energy can be neglected. In
such a situation, the larger ions (silver in this case) should
have lower activation energies.

It has been found from the microstructures of certain
oxide glass fibers subjected to sodium⇌silver ion exchange
treatment that the ion-exchanged layer consists of two phases
a silver deficient interconnected phase and a silver-rich
phase with broken interconnectivity.

Here we assume that a similar interconnected silver-
deficient phase and silver-rich phase with broken interconnecti-
vity exists in the silver rich layer of the ion exchanged glass
systems IG.

A mechanism for the switching of the ion-exchanged samples
to the highly conducting state is formulated on the assumption
that the ion exchanged layer consists of an interconnected silver
deficient phase and a silver rich layer with broken inter-
connectivity.

The switching of the ion-exchanged samples to the highly
conducting state under influence of a suitable combination of

electric field and temperature is believed to arise due to the formation of links between the disjointed portions of the silver rich phase.

The later seems to be a high conducting phase and leads to the formation of the high conducting state of the ion-exchanged sample. The forming mechanism is believed to arise due to an accelerated growth of the silver-rich under the influence of the applied electric field. Most of the voltage applied across the sample will be concentrated in the disjointed portions of the successive silver-rich regions because of their large conductivity values as compared to that of the intervening matrix phase. The growth takes place because of a lowering of the thermodynamic free energy due to the formation of the silver rich phase. The rate of growth u can be shown [Turnbull (28)] to be given by

$$u = \lambda \nu \exp(-\Delta F/kT) \qquad (3.1)$$

where λ - is the thickness of one atom layer of the growing phase,

ν - is the vibrating frequency of the ion

ΔF - is the activation energy for ionic diffusion across the interface between the two phases

T - is the temperature

It has been assumed in deriving equation (3.1) that the inequality

$v|\Delta F_v| \gg kT$ holds in the present case, v being the volume of ion and ΔF_v is the change in free energy per unit volume for the concerned phase transformation.

When electric field is applied, the expression for the growth rate will be

$$u_e = \lambda\nu\exp[-(\Delta F - e\lambda E)/kT] \qquad (3.2)$$

The critical growth rate at which the successive silver-rich regions touch each other can therefore be achieved either at a critical temperature T_c or at a critical field E_c. From eqns. (3.1) and (3.2) we get

$$E_c = \frac{F}{e\lambda}\left[1 - \frac{T}{T_c}\right] \qquad (3.3)$$

The decrease in E_c as a function of T as predicted by equation (3.3) is indeed observed experimentally as shown by Figure 3.17. It must be noted however that the experimental E_cs exhibit a nonlinear dependence on temperature. This could arise because of the presence of a range of ΔF values for the ionic movement from the matrix phase to the product phase. A distribution of activation energies for limited movements of cations in oxide glasses is known to exist [Taylor (29)].

The large concentration of silver ions in the newly formed interconnected silver-rich phase will lead to a situation where

some of the saddle point positions are also occupied by silver
ions. Ionic transport in such a case may arise due to a pair
of silver ions (one in the equilibrium site and the other in the
saddle point position) moving together under the influence of the
applied electric field. Such a mode of ionic migration will lead
to an extremely low value of activation energy. The experimental
data for the high conducting state of the ion-exchanged samples
suggest that a similar mechanism may be operative in the present
case. Fig. 3.18 to Fig. 3.20 gives the bulk resistivities of the
HIG glass system. Actually the conductivity is due to the migra-
tion of the silver ions in the silver-rich phase. So the actual
resistivities are the resistivities of the ion exchanged layers.
So considering only the ion-exchanged layers the resistivities
will be   x 10^{-3} times that of the given values.

Figs. 3.23 and 3.24 gives the steady state current-voltage
characteristics for the polarization cell $Ag/HIG_2/C^+$ and
$C/HIG_3/C$ cell respectively. Fig. 3.25 gives the conductivity-
time characteristics for the cell $C/HIG_3/C$. From these curves
it seems that the conductivity in the high conducting state is
ionic in nature.

CHAPTER IV

CONCLUSION

From the present studies it has been established that a new class of glasses based on SiO_4 tetrahedral network containing silver ions can be developed by subjecting the high-soda containing silica based glass to sodium silver ion exchange.

Another interesting outcome is the development of new high conducting glass systems which have almost negligible activation energy and high conductivity (10^{-2} to 10^{-1} (ohm-cm)$^{-1}$) at room temperature. These new high conducting glass systems have potential for futuristic applications in energy devices.

The highest conducting FIC glasses are AgI based and contain 700 to 80 mole % of silver and none of them is silica based.

It may be worth mentioning that the effect of electric field on the phase morphological change in oxide glasses is reported earlier [30]. It appears that the forming of the high conducting phases by the combined effect of electric field and temperature can be brought about in oxide glasses containing other monovalent ions e.g., lithium, copper (Chakraverty [31]) provided the virgin glass has the optimum microstructure.

REFERENCES

[1]   G. Warburg, Ann. Phys. 21 (1884) 622.

[2]   F. Bläber and A. Moser, Z. Elektrochem. 11 (1905) 593.

[3]   Z. Hauffe, Z. Elektrochem. 46 (1940) 348.

[4]   H. L. Tuller, D.P. Button and D.R. Uhlmann, J. Non-
      Crystalline Solids 40 (1980) 93.

[5]   N. Weber and J.T. Kummar, Proc. Ann. Power Sources Conf.
      21 (1967) 37.

[6]   D. Kunze in Fast Ion Transport in Solids ed. W. van Gool
      (North-Holland, American Elsevier, Amsterdam, 1973).

[7]   R.D. Armstrong, R.S. Bulmer and T. Dickinson, J. Solid St.
      Chem. 8 (1973) 219.

[8]   D. Chakravorty and A. Shrivastava, J. Phys. D: Appl. Phys 19
      (1986) 2185-2195.

[9]   N.F. Mott, Phil Mag. 19, 835 (1969); 24, 911, 935 (1971);
      Contemp. Phys., 10, 125 (1969).

[10] H. Fritzsche, J. Noncryst. Solids, 6, 49 (1971).

[11] N.K. Hindly, J. Noncryst. Solids, 5, 17 (1971).

[12] K. Tanaka, S. Iizima, M. Sugi and M. Kikuchi, Solid Stat.
      Commun. 8 (1970) 75.

[13] S.R. Ovshinsky, J. Non-Crystaline Solids 4 (1970) 538.

[14] N.F. Mott, Phil. Mag. 24 (1971) 911.

[15] Stevels, J.M.: 'The electrical properties of glass', In
      Handbook der Physik, 20 (1957) 380.

[16]   Taylor, H.E.: Ph.D. Thesis, University of Sheffield, England.

[17]   T. Minami, J. Non Cryst. Solids 73 (1985) 273-284.

[18]   A.M. Glass, J. Appl. Phys. 51 (1980) 3756.

[19]   D.P. Button, R.P. Tandom, H.L. Tuller and D.R. Uhlmann,
        J. Non-Crystalline Solids 42.

[20]   R.H. Dore us, Glass Science 1973, John Wiley and Sons, Inc.

[21]   Riebling, E.F., J. Chem. Phys. 55, 804 (1971).

[22]   Frischat G.H. Ionic Diffusion in Oxide Glasses, Trans. Tech.
        Publ. Aeder Monnedorf, Switzerland (1976).

[23]   Matousek, J. Silikaty 12, 73-78, 86-95 (1968), Matousek J.
        Nemec L: Sb. Vys. S.K. Chem. Technol. Praze Anorg: Chem.
        Technol. B16, 99-117, 1973.

[24]   Wagner, C.: International Committee of electrochemical
        Thermodynamics and Kinetics, Proc. 7th Meeting (1955).

[25]   D. Chakravorty, C.S. Vithlani and G.K. Mehta, J.Mat.Sci.
        13 (1978) 1438.

[28]*   Rawson H., Properties and Application of Glass (1984),
        Amsterdam Elsevier.

[26]   Chakravorty, D., Tiwari, A.N. and Goel P.S., 1972,
        Phys.Chem. Glasses 1391.

[27]   Stevels, J.M. 1957, The Electrical Property of Glasses in
        Handbuckder.

[29]   Turnbull, D., 1956, Phase Transformations Solid State
        Physics, Volume 3 (NY Academic Press).

[29]   Taylor, H.E., 1957, J.Soc. Glass Tech. 14350.

[30]   DeVekcy and Majumdar 1970, Nature 25, 172.

[31]   Chakravorty D, Shjuttleworth and Gaskell, P.H., 1975,
        J. Mater. Sci. 10 799.

MSP-1987-M-MAT-ELE